



# Effective Field Theory (EFT) limits from ATLAS and CMS

Mark Owen  
On behalf of ATLAS & CMS  
The University of Glasgow

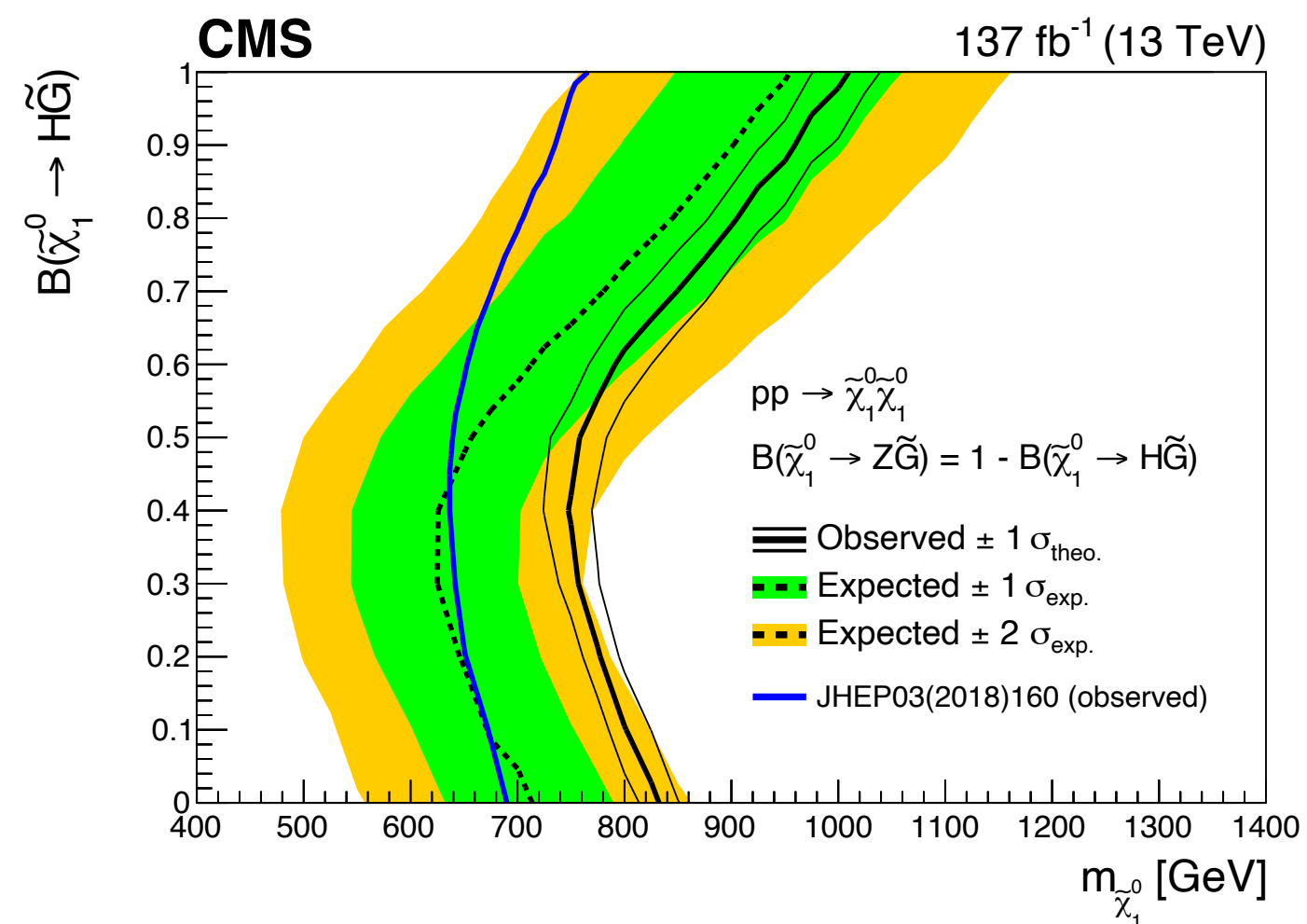
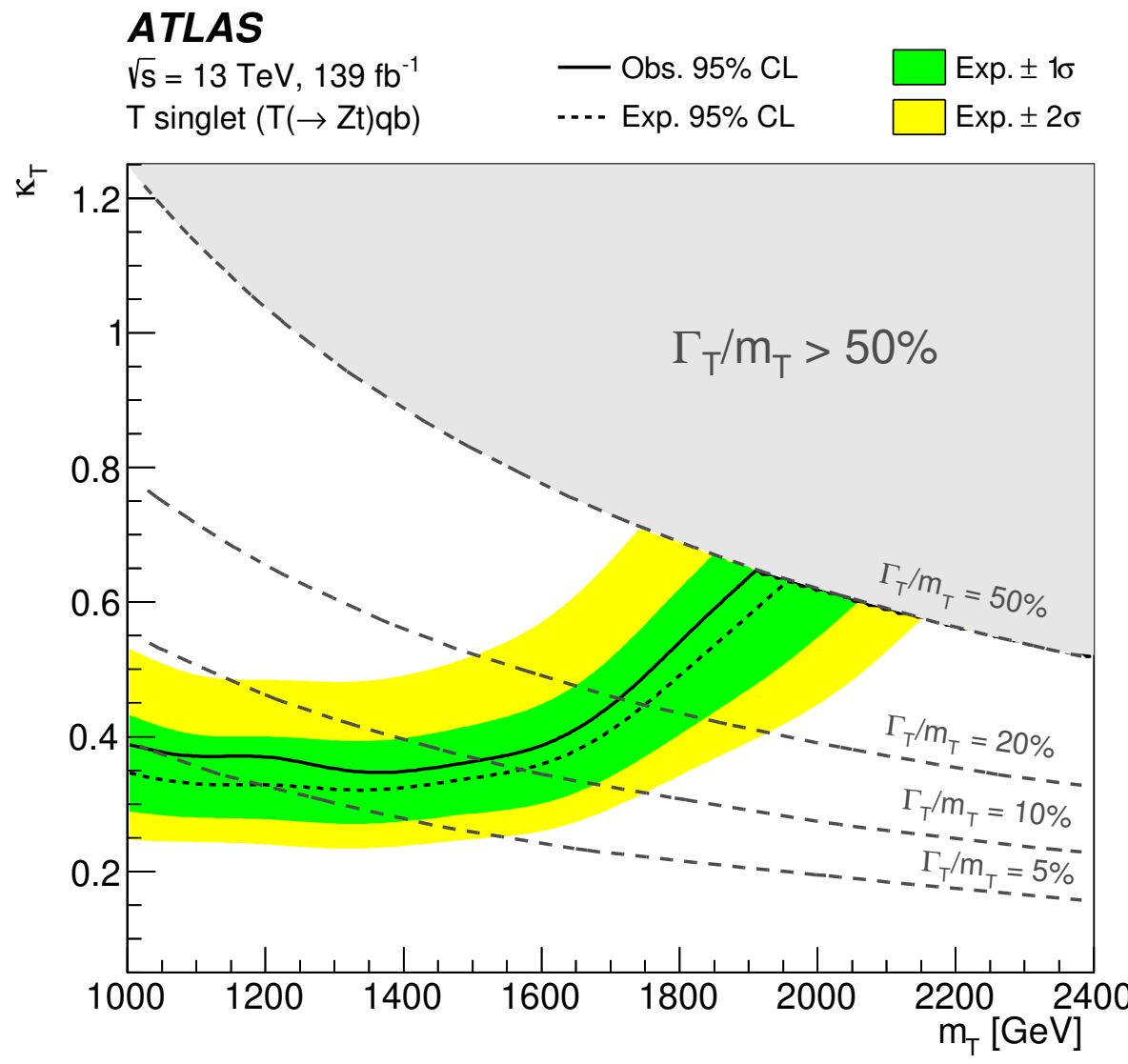
Moriond EW 2024

# Outline

- Why (SM)EFT for ATLAS and CMS?
- Highlights of recent SMEFT limits:
  - CMS  $\gamma\gamma \rightarrow \tau\tau$
  - ATLAS WWjj
  - ATLAS  $hh \rightarrow bb\gamma\gamma$
  - ATLAS  $t\bar{t}Z + t\bar{t}\gamma$
  - CMS tt + leptons
- Summary

# New physics limits at the LHC

- Huge programme of dedicated searches for new particles / forces:



# SM Effective field theory

- New physics could be at such a high energy scale that we cannot see the new resonances at the LHC.
- New particles will still impact LHC measurements - parameterise this with an effective field theory:

$$\mathcal{L}_{\text{SMEFT}} = \mathcal{L}_{\text{SM}} + \sum_i \frac{c_i^{(5)}}{\Lambda} O_i^{(5)} + \sum_i \frac{c_i^{(6)}}{\Lambda^2} O_i^{(6)} + \dots$$

$O_i^{(n)}$ : operator of dimension n (obeying SM symmetries)

$c_i^{(n)}$ : Wilson coefficient for  $O_i^{(n)}$

$\Lambda$ : energy scale of new physics

# SM Effective field theory

- New physics could be at such a high energy scale that we cannot see the new resonances at the LHC.
- New particles will still impact LHC measurements - parameterise this with an effective field theory:

$$\mathcal{L}_{\text{SMEFT}} = \mathcal{L}_{\text{SM}} + \sum_i \frac{c_i^{(5)}}{\Lambda} O_i^{(5)} + \sum_i \frac{c_i^{(6)}}{\Lambda^2} O_i^{(6)} + \dots$$

$O_i^{(n)}$ : operator of dimension n (obeying SM symmetries)

$c_i^{(n)}$ : Wilson coefficient for  $O_i^{(n)}$

$\Lambda$ : energy scale of new physics

- If  $\Lambda \gg E$ , can truncate series at e.g. n=6.
- One n=5 operator violates L conservation and can generate neutrino mass - not relevant for LHC studies.
- For n=6, Warsaw basis [[JHEP 10 \(2010\) 085](#)] often used to define a complete set of independent operators - 59 operators for CP-even and restricted-flavour scenario.

# Effect on observables

$$\sigma = |\mathcal{A}_{\text{SM}}|^2 + \sum_i \frac{c_i^{(6)}}{\Lambda^2} 2\text{Re}\left(\mathcal{A}_i^{(6)} \mathcal{A}_{\text{SM}}^*\right) + \sum_i \frac{\left(c_i^{(6)}\right)^2}{\Lambda^4} \left|\mathcal{A}_i^{(6)}\right|^2 + \sum_{i < j} \frac{c_i^{(6)} c_j^{(6)}}{\Lambda^4} 2\text{Re}\left(\mathcal{A}_i^{(6)} \mathcal{A}_j^{(6)*}\right)$$

# Effect on observables

$$\sigma = |\mathcal{A}_{\text{SM}}|^2 + \sum_i \frac{c_i^{(6)}}{\Lambda^2} 2\text{Re}(\mathcal{A}_i^{(6)} \mathcal{A}_{\text{SM}}^*) + \sum_i \frac{(c_i^{(6)})^2}{\Lambda^4} |\mathcal{A}_i^{(6)}|^2 + \sum_{i < j} \frac{c_i^{(6)} c_j^{(6)}}{\Lambda^4} 2\text{Re}(\mathcal{A}_i^{(6)} \mathcal{A}_j^{(6)*})$$

↑  
SM

# Effect on observables

$$\sigma = |\mathcal{A}_{\text{SM}}|^2 + \sum_i \frac{c_i^{(6)}}{\Lambda^2} 2\text{Re}(\mathcal{A}_i^{(6)} \mathcal{A}_{\text{SM}}^*) + \sum_i \frac{(c_i^{(6)})^2}{\Lambda^4} |\mathcal{A}_i^{(6)}|^2 + \sum_{i < j} \frac{c_i^{(6)} c_j^{(6)}}{\Lambda^4} 2\text{Re}(\mathcal{A}_i^{(6)} \mathcal{A}_j^{(6)*})$$

SM

Interference of SM and NP

```
graph TD; A["σ = |ASM|2 + ..."] --> B["SM"]; A --> C["Interference of SM and NP"]; A --> D["NP"]
```

# Effect on observables

$$\sigma = |\mathcal{A}_{\text{SM}}|^2 + \sum_i \frac{c_i^{(6)}}{\Lambda^2} 2\text{Re}(\mathcal{A}_i^{(6)} \mathcal{A}_{\text{SM}}^*) + \sum_i \frac{(c_i^{(6)})^2}{\Lambda^4} |\mathcal{A}_i^{(6)}|^2 + \sum_{i < j} \frac{c_i^{(6)} c_j^{(6)}}{\Lambda^4} 2\text{Re}(\mathcal{A}_i^{(6)} \mathcal{A}_j^{(6)*})$$

The diagram illustrates the decomposition of the total cross-section  $\sigma$  into three components. The first term,  $|\mathcal{A}_{\text{SM}}|^2$ , is labeled 'SM' with an arrow pointing to it. The second term, involving the sum over  $i$  of  $\frac{c_i^{(6)}}{\Lambda^2} 2\text{Re}(\mathcal{A}_i^{(6)} \mathcal{A}_{\text{SM}}^*)$ , is labeled 'Interference of SM and NP' with an arrow pointing to it. The third term, involving the sum over  $i$  of  $\frac{(c_i^{(6)})^2}{\Lambda^4} |\mathcal{A}_i^{(6)}|^2$ , is labeled 'Pure NP' with an arrow pointing to it. A fourth term, involving the sum over  $i < j$  of  $\frac{c_i^{(6)} c_j^{(6)}}{\Lambda^4} 2\text{Re}(\mathcal{A}_i^{(6)} \mathcal{A}_j^{(6)*})$ , is also present but lacks a specific label.

# Effect on observables

$$\sigma = |\mathcal{A}_{\text{SM}}|^2 + \sum_i \frac{c_i^{(6)}}{\Lambda^2} 2\text{Re}(\mathcal{A}_i^{(6)} \mathcal{A}_{\text{SM}}^*) + \sum_i \frac{(c_i^{(6)})^2}{\Lambda^4} |\mathcal{A}_i^{(6)}|^2 + \sum_{i < j} \frac{c_i^{(6)} c_j^{(6)}}{\Lambda^4} 2\text{Re}(\mathcal{A}_i^{(6)} \mathcal{A}_j^{(6)*})$$

SM

Interference of SM and NP

Pure NP

The diagram illustrates the decomposition of the total cross-section  $\sigma$  into three components. The first component, labeled 'SM', is represented by an upward arrow pointing to the term  $|\mathcal{A}_{\text{SM}}|^2$ . The second component, labeled 'Interference of SM and NP', is represented by a double-headed arrow pointing to the term  $\sum_i \frac{c_i^{(6)}}{\Lambda^2} 2\text{Re}(\mathcal{A}_i^{(6)} \mathcal{A}_{\text{SM}}^*)$ . The third component, labeled 'Pure NP', is represented by a downward arrow pointing to the term  $\sum_i \frac{(c_i^{(6)})^2}{\Lambda^4} |\mathcal{A}_i^{(6)}|^2 + \sum_{i < j} \frac{c_i^{(6)} c_j^{(6)}}{\Lambda^4} 2\text{Re}(\mathcal{A}_i^{(6)} \mathcal{A}_j^{(6)*})$ .

$$\sigma = \sigma_{\text{SM}} + \sum_i \frac{c_i}{\Lambda^2} p_i + \sum_i \frac{c_i^2}{\Lambda^4} p_{2,i} + \sum_{i < j} \frac{c_i c_j}{\Lambda^4} p_{ij}$$

# Effect on observables

$$\sigma = |\mathcal{A}_{\text{SM}}|^2 + \sum_i \frac{c_i^{(6)}}{\Lambda^2} 2\text{Re}(\mathcal{A}_i^{(6)} \mathcal{A}_{\text{SM}}^*) + \sum_i \frac{(c_i^{(6)})^2}{\Lambda^4} |\mathcal{A}_i^{(6)}|^2 + \sum_{i < j} \frac{c_i^{(6)} c_j^{(6)}}{\Lambda^4} 2\text{Re}(\mathcal{A}_i^{(6)} \mathcal{A}_j^{(6)*})$$

The diagram illustrates the decomposition of the total cross-section  $\sigma$  into three components. The first term,  $|\mathcal{A}_{\text{SM}}|^2$ , is labeled 'SM'. The second term, involving the sum over  $i$  of  $\frac{c_i^{(6)}}{\Lambda^2} 2\text{Re}(\mathcal{A}_i^{(6)} \mathcal{A}_{\text{SM}}^*)$ , is labeled 'Interference of SM and NP'. The third term, involving the sum over  $i$  of  $\frac{(c_i^{(6)})^2}{\Lambda^4} |\mathcal{A}_i^{(6)}|^2$ , is labeled 'Pure NP'. Arrows point from each term to its corresponding label.

$$\sigma = \sigma_{\text{SM}} + \sum_i \frac{c_i}{\Lambda^2} p_i + \sum_i \frac{c_i^2}{\Lambda^4} p_{2,i} + \sum_{i < j} \frac{c_i c_j}{\Lambda^4} p_{ij}$$

- Just need quadratic parameterisation in  $\frac{c_i}{\Lambda^2}$  & a measurement can be used to constrain  $c_i$ .
- Want observables that: (i) have large  $p_i/\sigma_{\text{SM}}$  (ii) we can measure precisely.
- Caveat: dimension 8 operators also enter at  $\frac{1}{\Lambda^4}$ , but are often neglected.

# Effect on observables

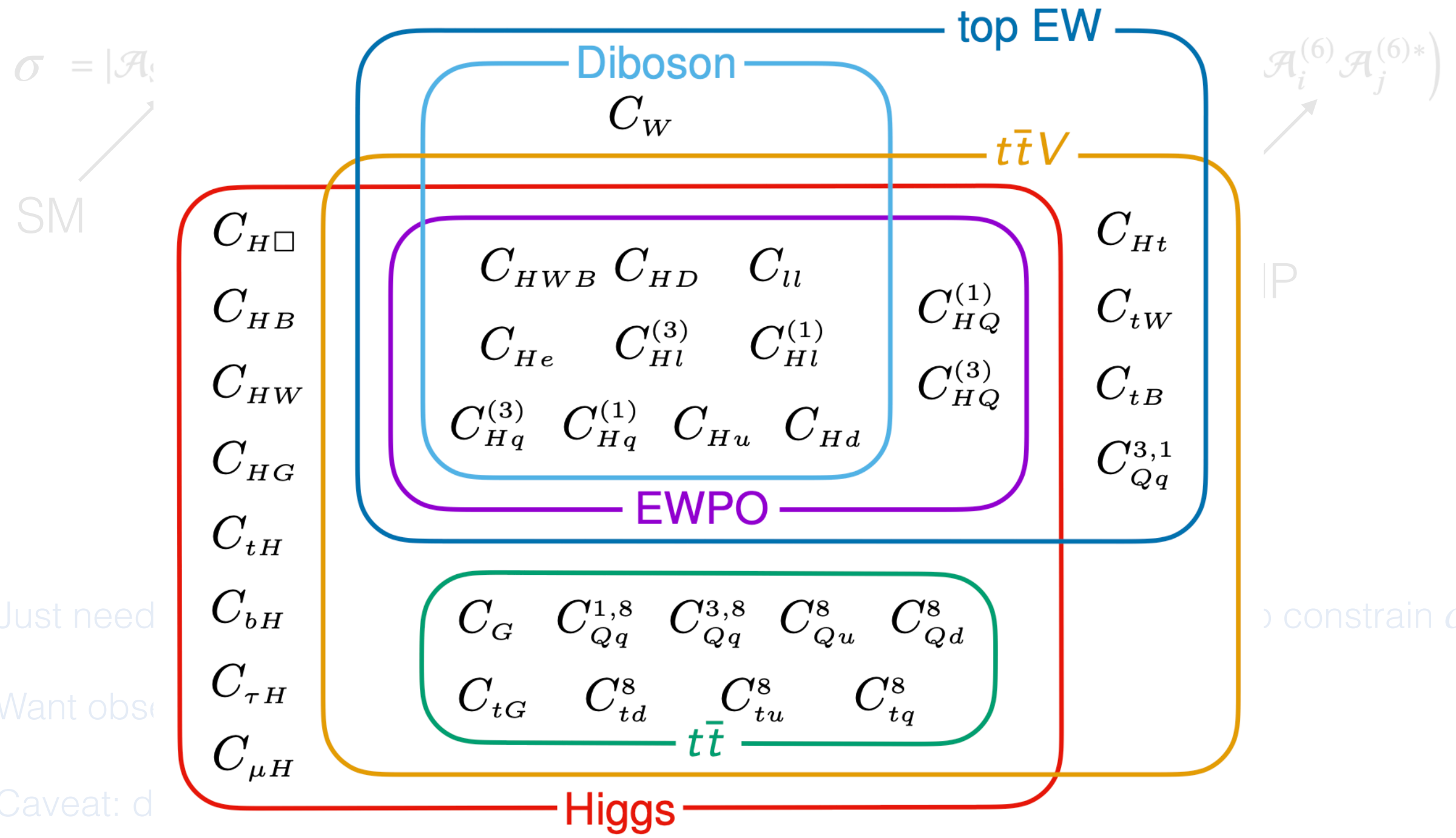
$$\sigma = |\mathcal{A}_{\text{SM}}|^2 + \sum_i \frac{c_i^{(6)}}{\Lambda^2} 2\text{Re}(\mathcal{A}_i^{(6)} \mathcal{A}_{\text{SM}}^*) + \sum_i \frac{(c_i^{(6)})^2}{\Lambda^4} |\mathcal{A}_i^{(6)}|^2 + \sum_{i < j} \frac{c_i^{(6)} c_j^{(6)}}{\Lambda^4} 2\text{Re}(\mathcal{A}_i^{(6)} \mathcal{A}_j^{(6)*})$$

The diagram illustrates the decomposition of the total cross-section  $\sigma$  into three components: SM, Interference of SM and NP, and Pure NP. Arrows point from each term in the equation to its corresponding component in the diagram.

$$\sigma = \sigma_{\text{SM}} + \sum_i \frac{c_i}{\Lambda^2} p_i + \sum_i \frac{c_i^2}{\Lambda^4} p_{2,i} + \sum_{i < j} \frac{c_i c_j}{\Lambda^4} p_{ij}$$

- Just need quadratic parameterisation in  $\frac{c_i}{\Lambda^2}$  & a measurement can be used to constrain  $c_i$ .
- Want observables that: (i) have large  $p_i/\sigma_{\text{SM}}$  (ii) we can measure precisely.
- Caveat: dimension 8 operators also enter at  $\frac{1}{\Lambda^4}$ , but are often neglected.
- Aim for global fits of many operators with many input physics measurements.

# Effect on observables



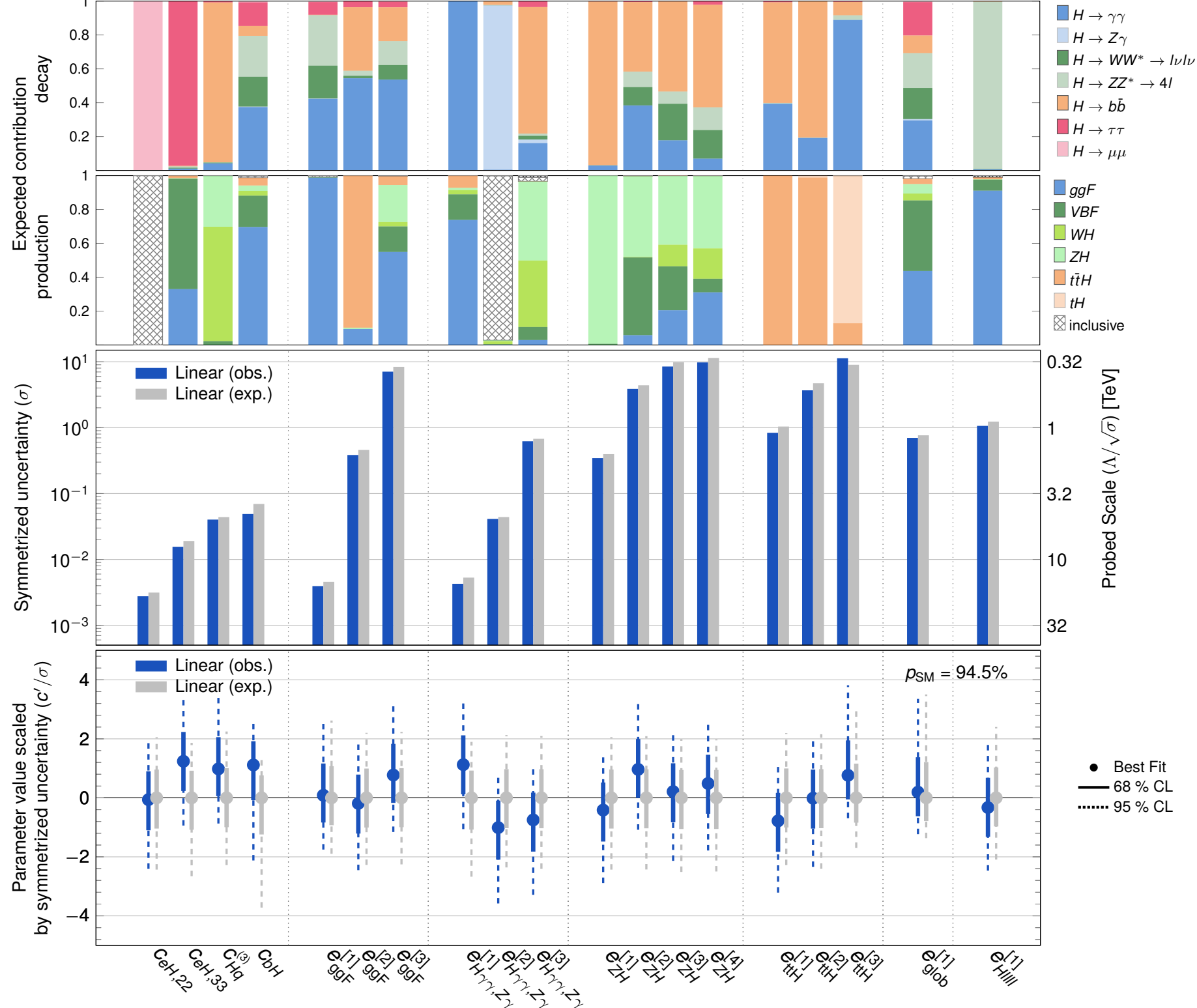
- Just need to constrain  $c_i$ .
- Want observational constraints.
- Caveat: don't have enough constraints.
- Aim for global fits of many operators with many input physics measurements.

# Combined Higgs fit

ATLAS

$\sqrt{s} = 13 \text{ TeV}, 139 \text{ fb}^{-1}, m_H = 125.09 \text{ GeV}$

SMEFT  $\Lambda = 1 \text{ TeV}$



arXiv:2402.05742



# CMS $pp(\gamma\gamma) \rightarrow \tau\tau$

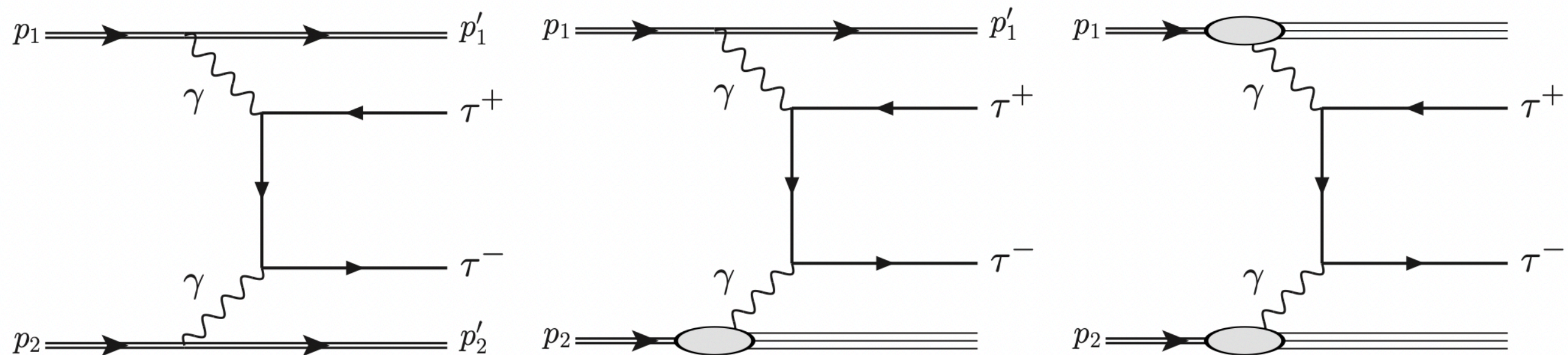
Other recent exclusive studies:

CMS  $\gamma\gamma \rightarrow WW/ZZ$  [JHEP 07 \(2023\) 229](#)

ATLAS and CMS PbPb( $\gamma\gamma$ )  $\rightarrow \tau\tau$  [PRL 131 \(2023\) 151802](#), [PRL 131 \(2023\) 151803](#)

# CMS $\gamma\gamma \rightarrow \tau\tau$

- Use LHC as a photon collider:



- The process probes the magnetic ( $a_\tau$ ) and electric ( $d_\tau$ ) dipole moments of the tau lepton, which are related to SMEFT operators:

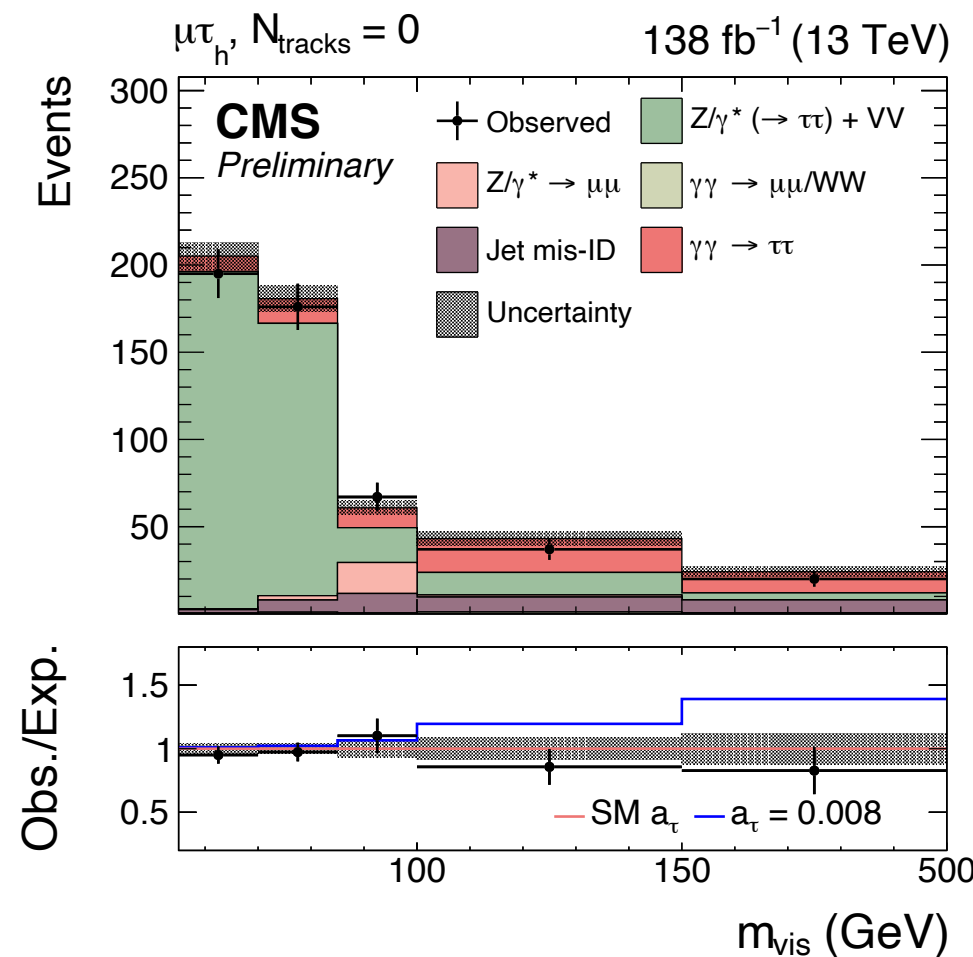
$$\delta a_\tau = \frac{2m_\tau}{e} \frac{\sqrt{2}v}{\Lambda^2} \text{Re} [C_{\tau\gamma}]$$

$$\delta d_\tau = \frac{\sqrt{2}v}{\Lambda^2} \text{Im} [C_{\tau\gamma}]$$

$$C_{\tau\gamma} = (\cos\theta_W C_{\tau B} - \sin\theta_W C_{\tau W})$$

# CMS $\gamma\gamma \rightarrow \tau\tau$

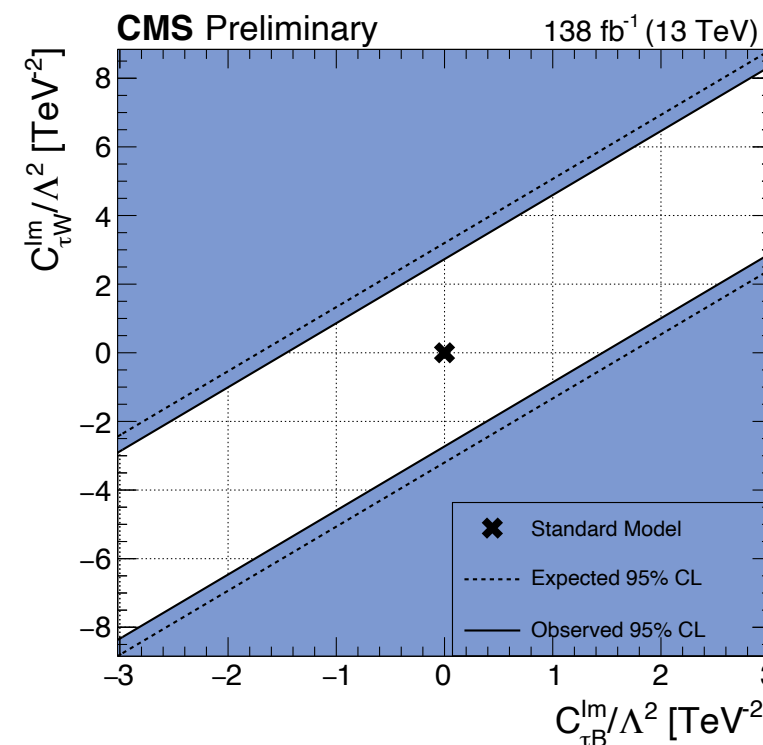
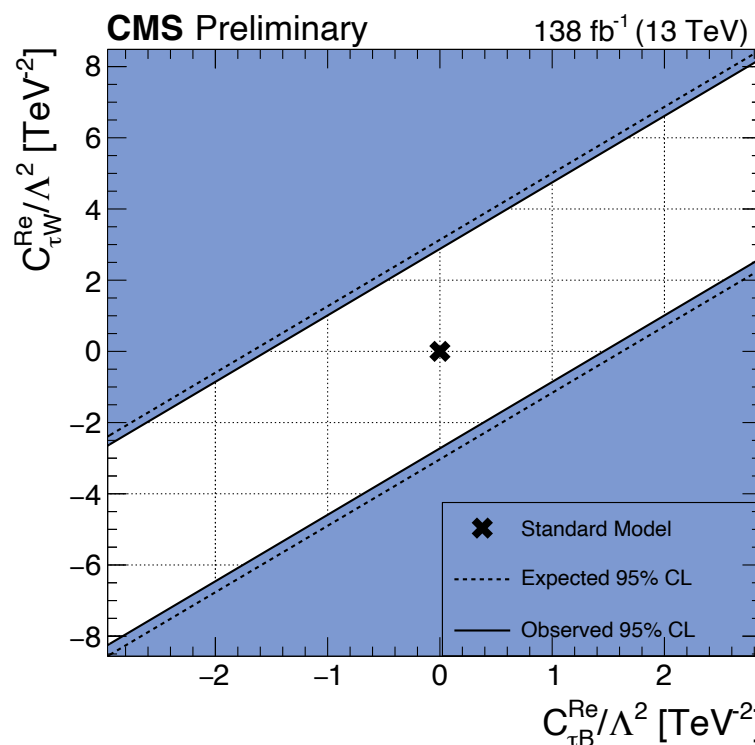
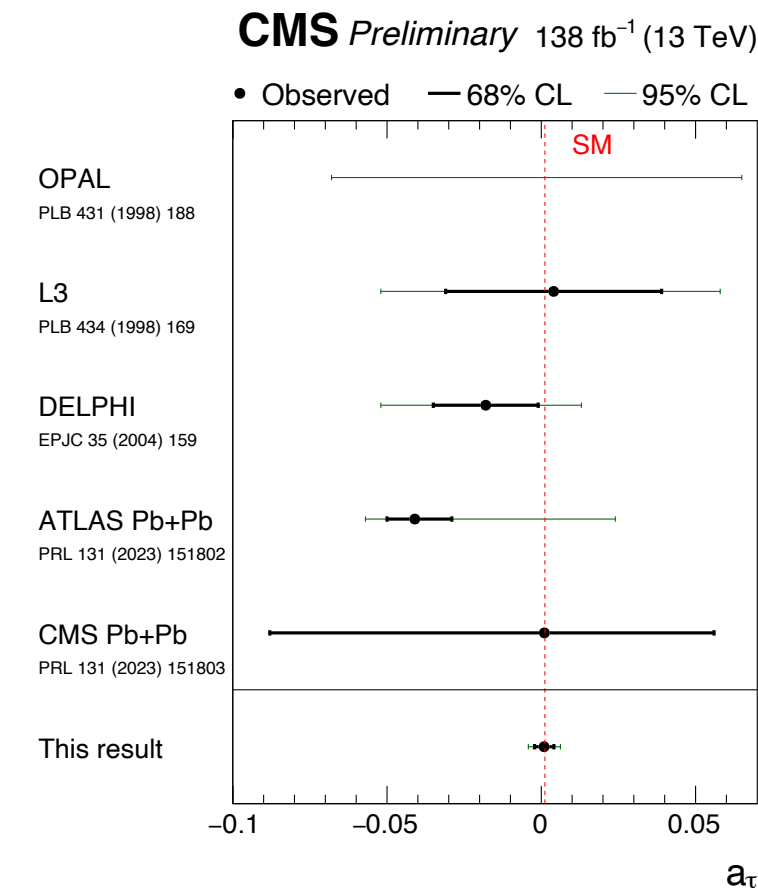
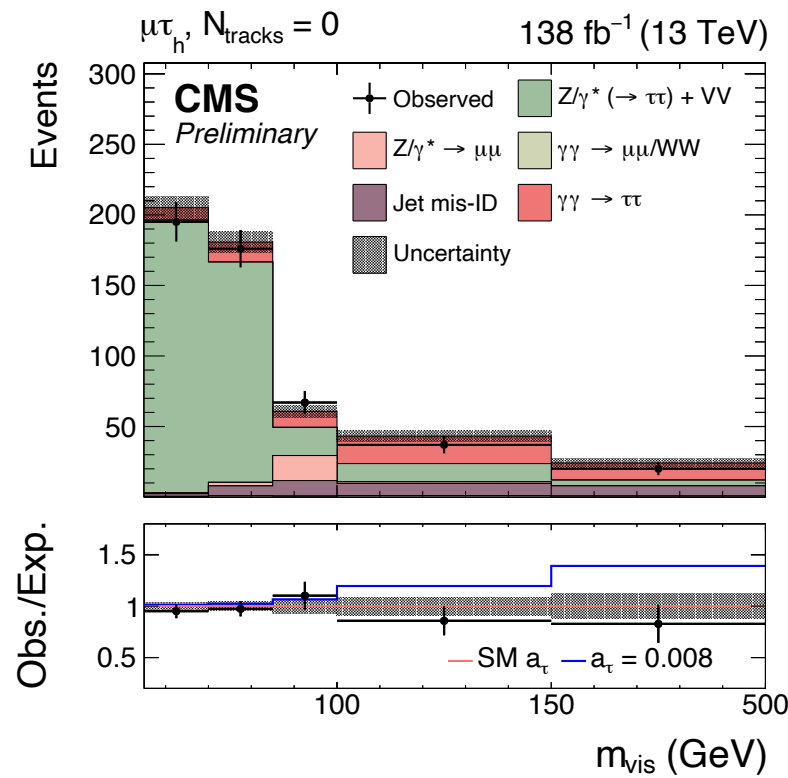
- Search for  $e\mu, e\tau_h, \mu\tau_h, \tau_h\tau_h$  channels.
- “Exclusivity” requirement of maximum 1 track close to the tau decay products is crucial to select di-photon production.
- Invariant mass of tau decay products provides observable sensitive of new physics:



First observation ( $5.3\sigma$ ) of  
 $pp(\gamma\gamma) \rightarrow \tau\tau$ .

CMS-PAS-SMP-23-005

# CMS $\gamma\gamma \rightarrow \tau\tau$ limits





# ATLAS $W^\pm W^\pm jj$

Other recent diboson EFT studies:

ATLAS  $W\gamma jj$  [arXiv:2403.02809](#)

ATLAS  $WZjj$  [arXiv:2403.15296](#)

ATLAS  $ZZ$  [arXiv:2310.04350](#)

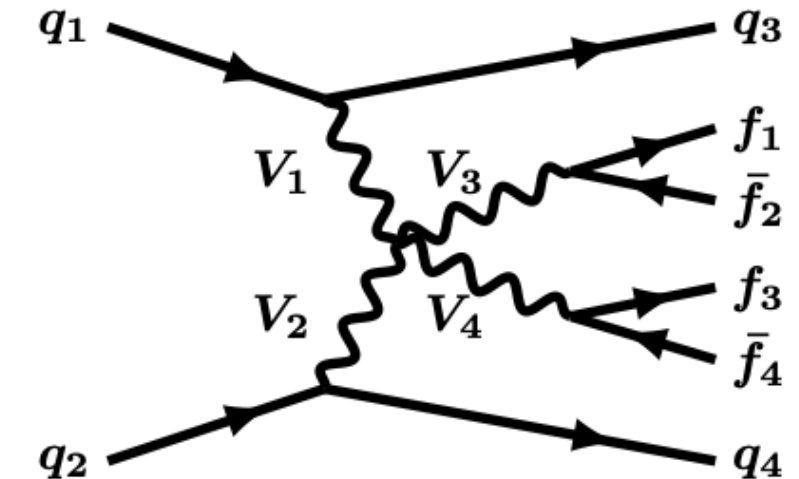
CMS  $W\gamma jj$  [PRD 108 \(2023\) 032017](#)

CMS exclusive  $WW$ ,  $ZZ$  [JHEP 07 \(2023\) 229](#)

[arXiv:2312.00420](#)

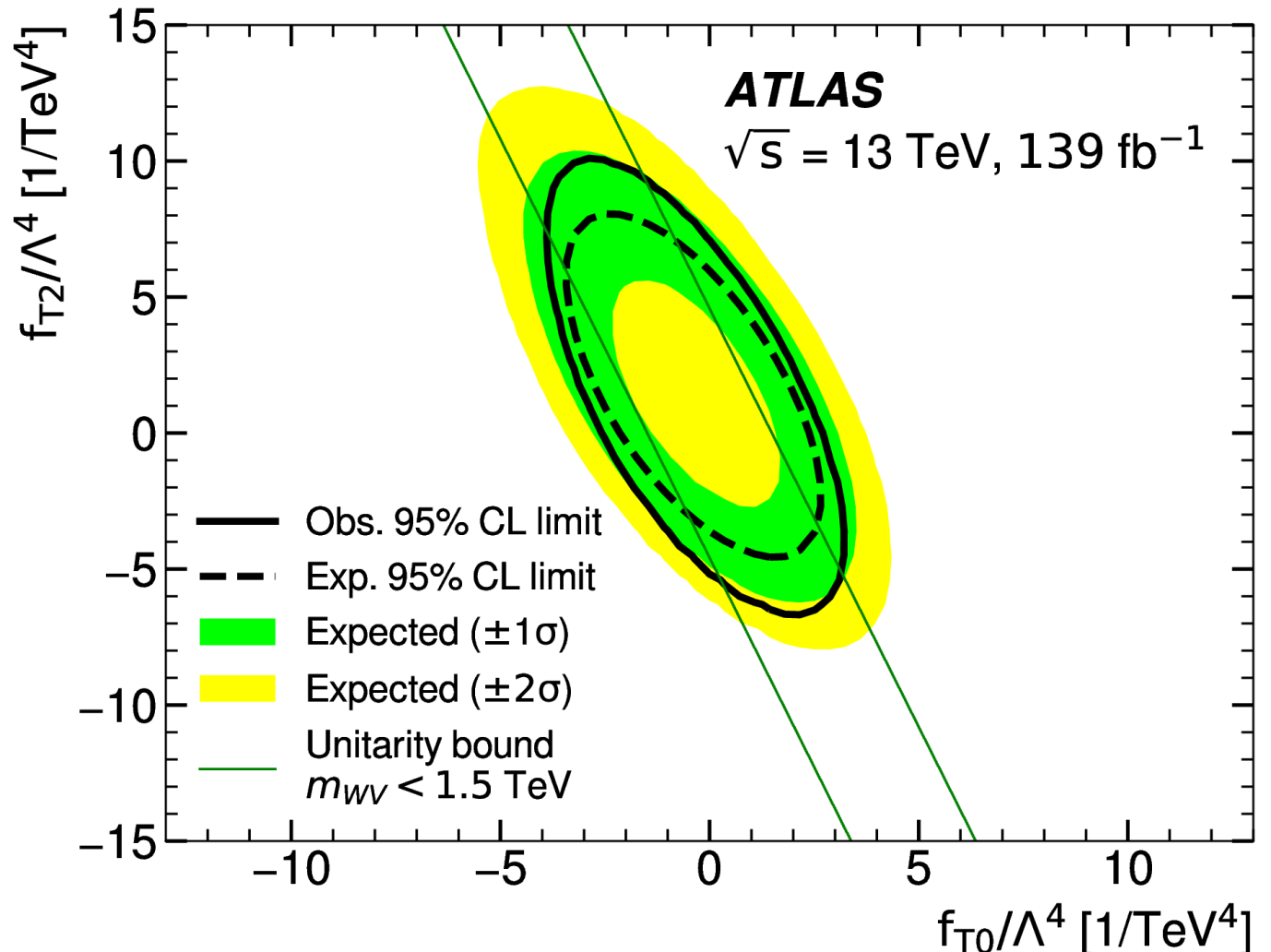
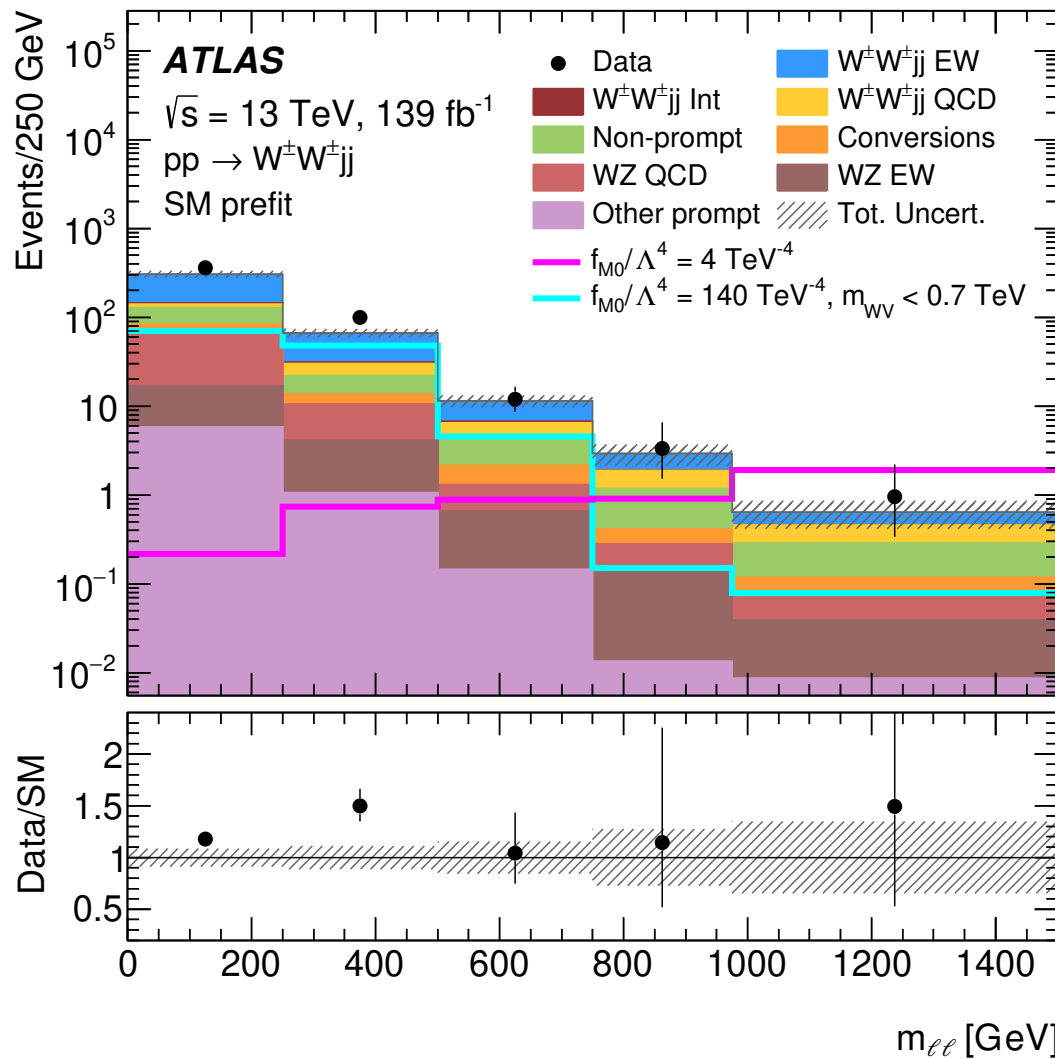
# ATLAS $W^\pm W^\pm jj$

- Same-sign W boson production possible in SM via triple & quartic gauge boson vertices and Higgs exchange.
- Contributions to quartic vertex (and not triple vertex) appear first at dimension 8 in SMEFT.
- Analysis selects  $\ell^\pm \ell^\pm jj$  events consistent with vector-boson scattering - high  $m(jj)$ , large  $\Delta y(jj)$ .
- Differential cross-section are measured in the paper, but EFT limits done by direct fit to the reconstructed  $m(\ell\ell)$  distribution and two control regions.
- 8 operators considered, either in 1D or 2D fits.



[arXiv:2312.00420](https://arxiv.org/abs/2312.00420)

# ATLAS $W^\pm W^\pm jj$



- EFT predictions can violate unitarity - this is implemented in the limits by applying a WV invariant mass requirement on the signal which varies according to the sensitivity.
- Competitive limits with earlier CMS measurement [[PLB 809 \(2020\) 135710](#)].

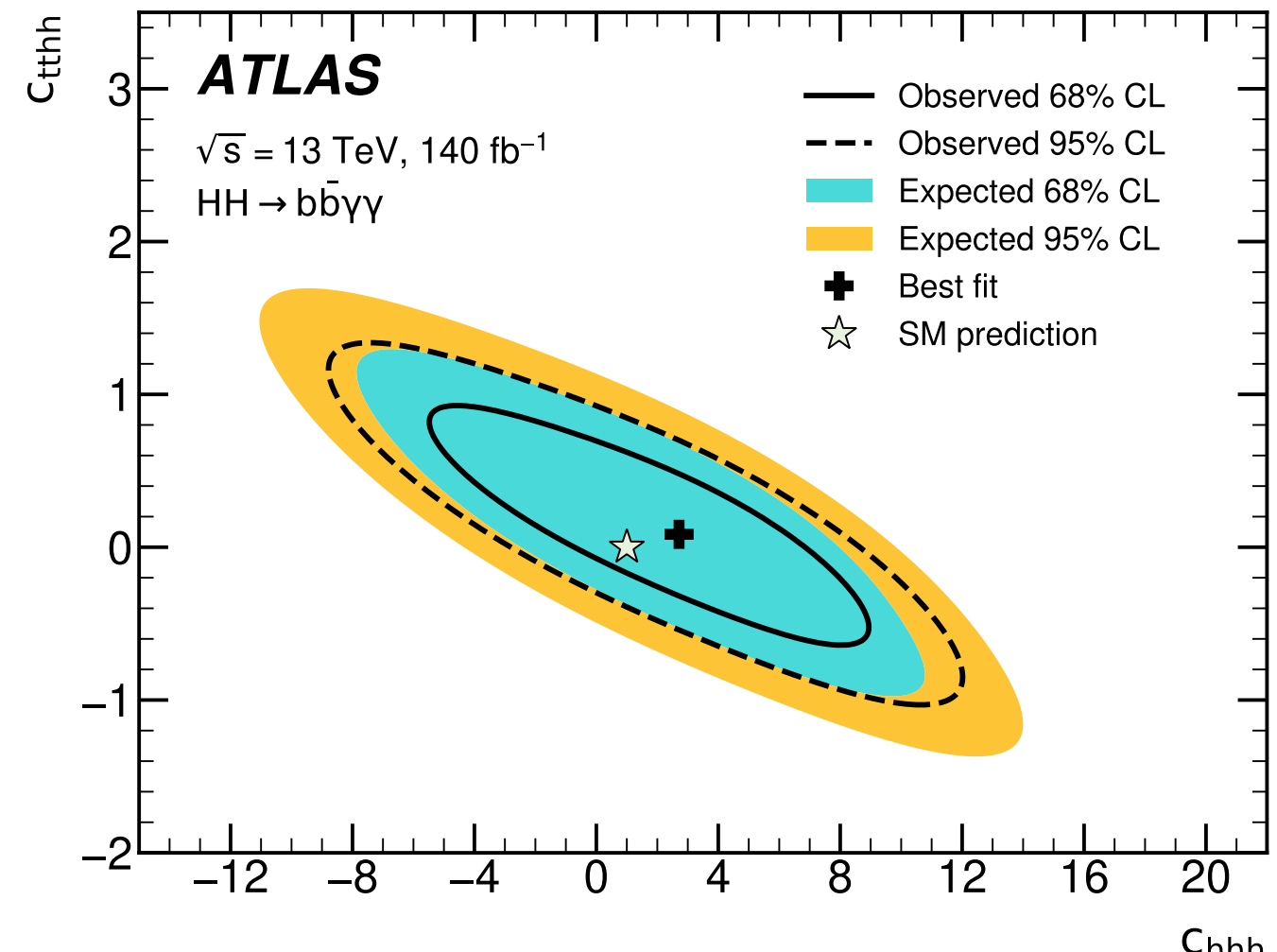
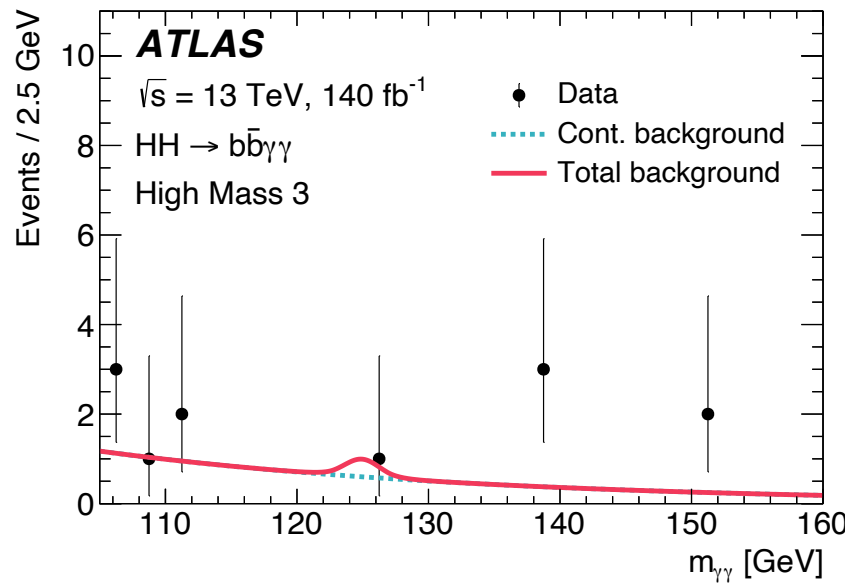
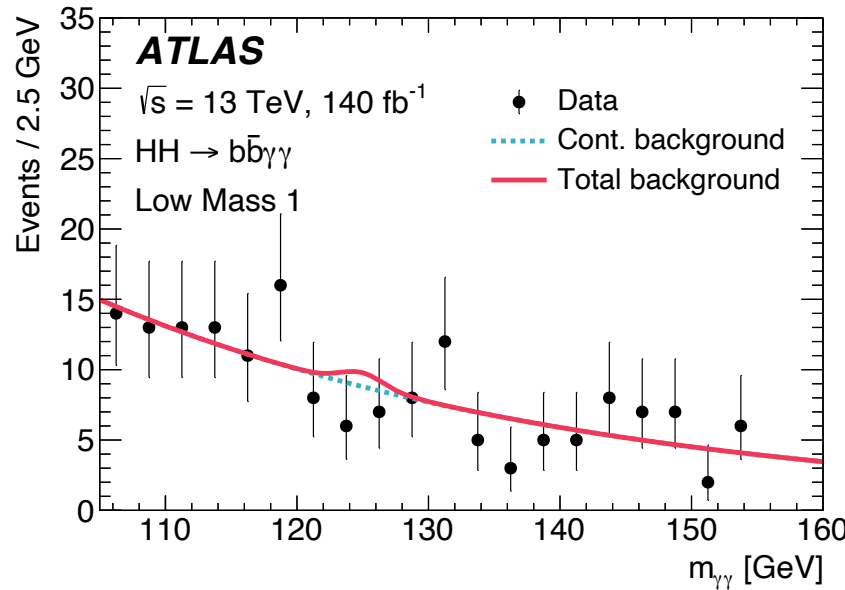
ATLAS  $hh \rightarrow b b \gamma\gamma$

# ATLAS $hh \rightarrow bb\gamma\gamma$

- Not yet at SM sensitivity for  $hh$ , but can probe non-SM contributions.
- Interesting case, where alternate HEFT Lagrangian formalism is used, in addition to SMEFT interpretation.
  - Couplings of HH to fermions / gluons decoupled from H to fermions / gluons, test  $c_{hhh}$ ,  $c_{tthh}$  and  $c_{gghh}$ .
  - Analysis separates events by  $m^*(bb\gamma\gamma)$  - different operators contribute to different regions.

$$m^*(bb\gamma\gamma) = m(bb\gamma\gamma) - (m(bb) - m_H) - (m(\gamma\gamma) - m_H)$$

# ATLAS $hh \rightarrow b\bar{b}\gamma\gamma$

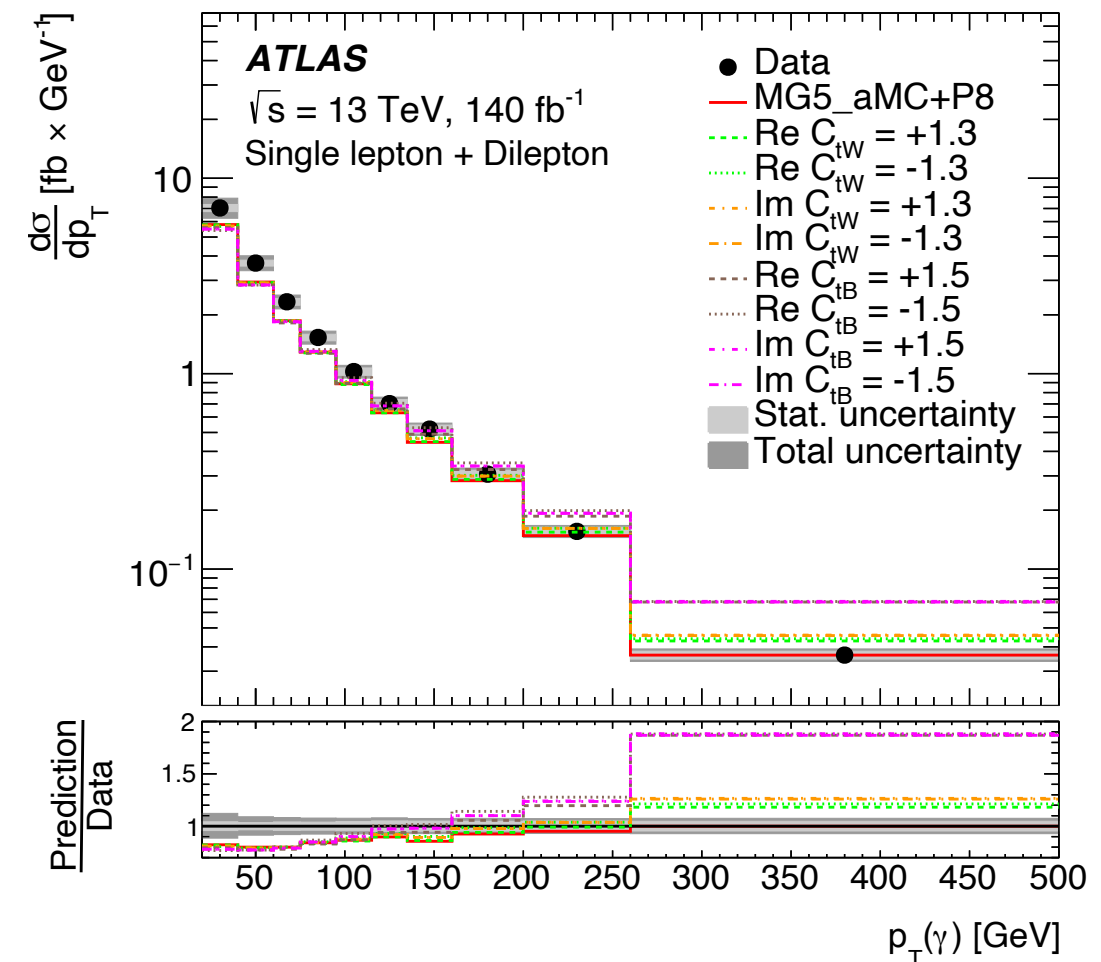
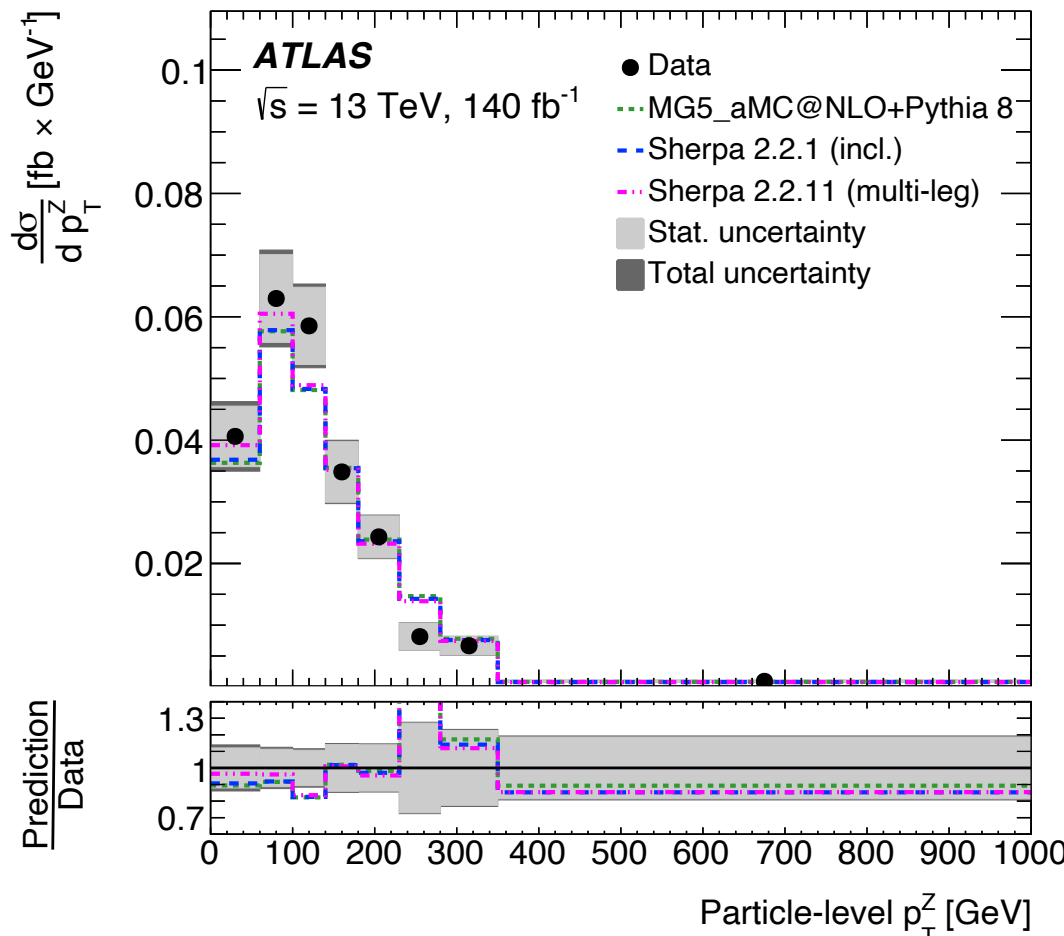


- No deviation from SM.

ATLAS  $t\bar{t}Z + t\bar{t}\gamma$

# ATLAS $t\bar{t}Z + t\bar{t}\gamma$

- Recent differential cross-section measurements of  $t\bar{t}Z$  and  $t\bar{t}\gamma$  production:



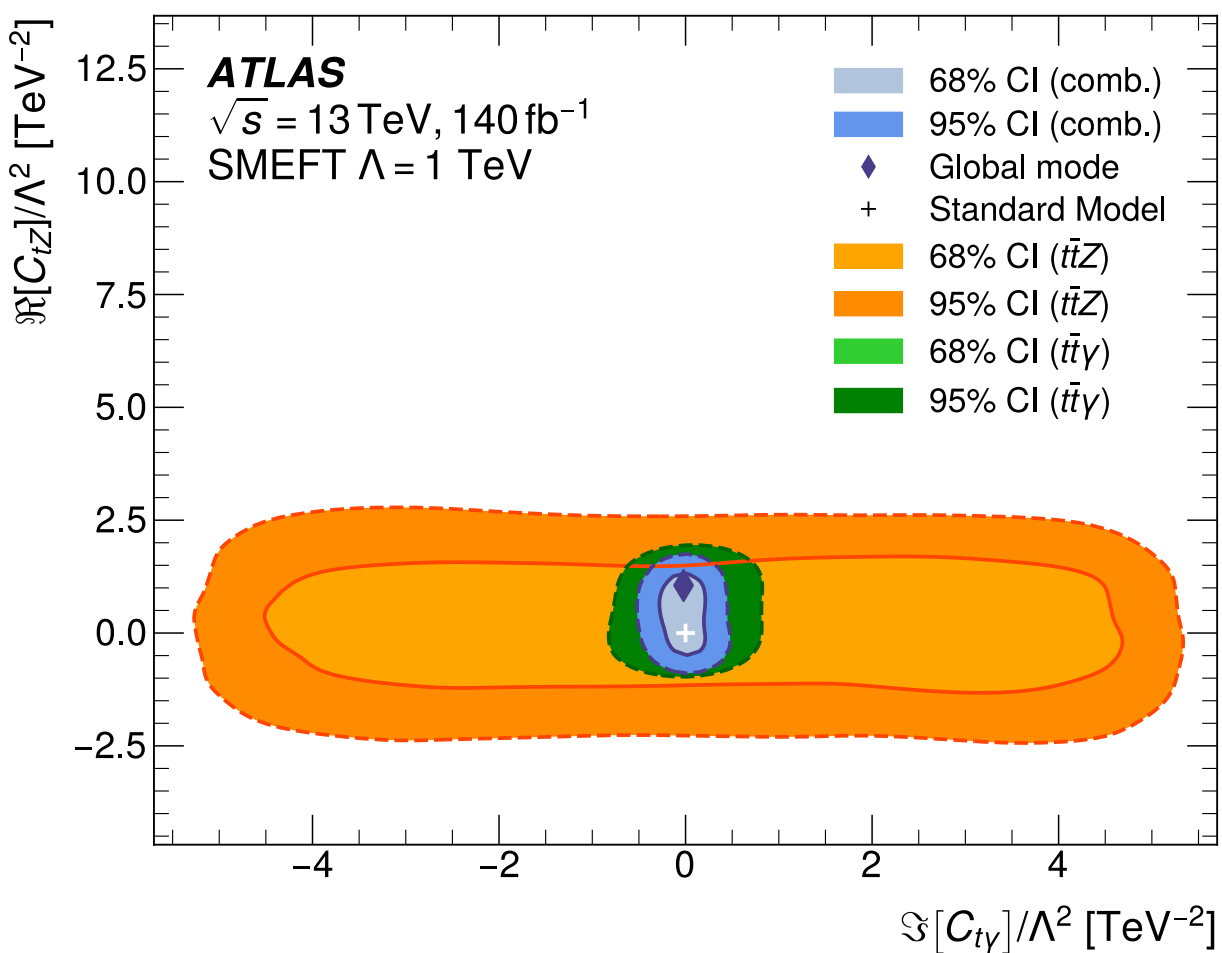
Simultaneous EFT fit to the two distributions,  
with two complex WC:  $C_{tZ}, C_{t\gamma}$

$$C_{tZ} = \cos \theta_W C_{tW} - \sin \theta_W C_{tB}$$

$$C_{t\gamma} = \sin \theta_W C_{tW} + \cos \theta_W C_{tB}$$

# ATLAS $t\bar{t}Z + t\bar{t}\gamma$

- Example limit (other WC are marginalised over):



Combination of  
measurements significantly  
improves sensitivity.

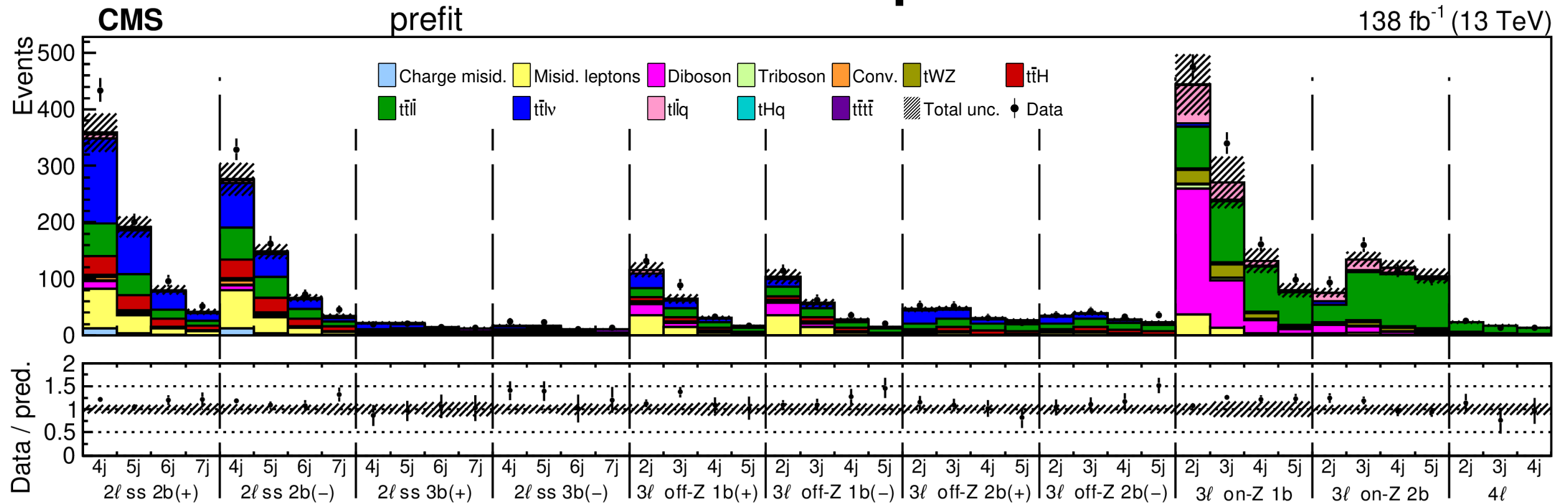


# CMS tt + leptons

# CMS $t\bar{t}$ + leptons

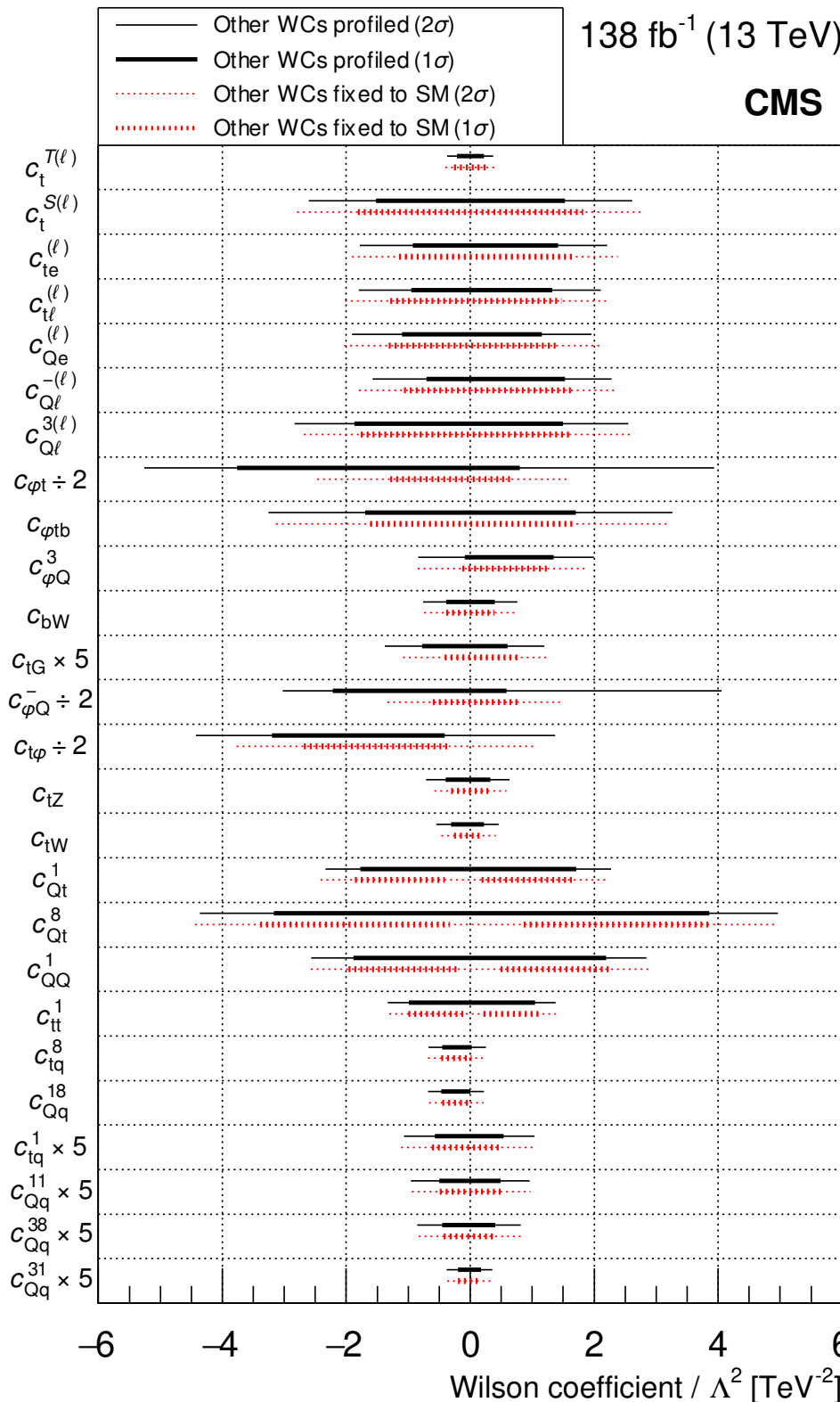
- Multiple physics processes can lead to  $t\bar{t}$  + additional leptons:  
 $t\bar{t}H, t\bar{t}Z, t\bar{t}W, t\bar{t}t\bar{t}, tZq, tHq$ .
  - Single SMEFT operator can affect many of the processes.
- Analysis looks at events with 2 (same charge), 3 or 4 leptons, at least 2 jets (1 b-jet).
  - Events are subdivided according to number of jets, b-jets and lepton charge.
- Observables:
  - Most ttZ like events:  $p_T(Z \rightarrow \ell^+\ell^-)$ .
  - Others:  $p_T$  of pair of jet / lepton 4-vectors with highest  $p_T$ .

# CMS tt + leptons



- EFT fits to reconstructed level data, 26 EFT operators are considered.
- Fits done with either:
  - All Wilson coefficients free-floating (profiled)
  - Only one / two are free and others are fixed to 0.

# CMS tt + leptons



- Powerful analysis - limits not degrading going from individual (red) to profiled (black) fits.
- Direct comparisons to ATLAS result challenging due to operator definitions / sets.

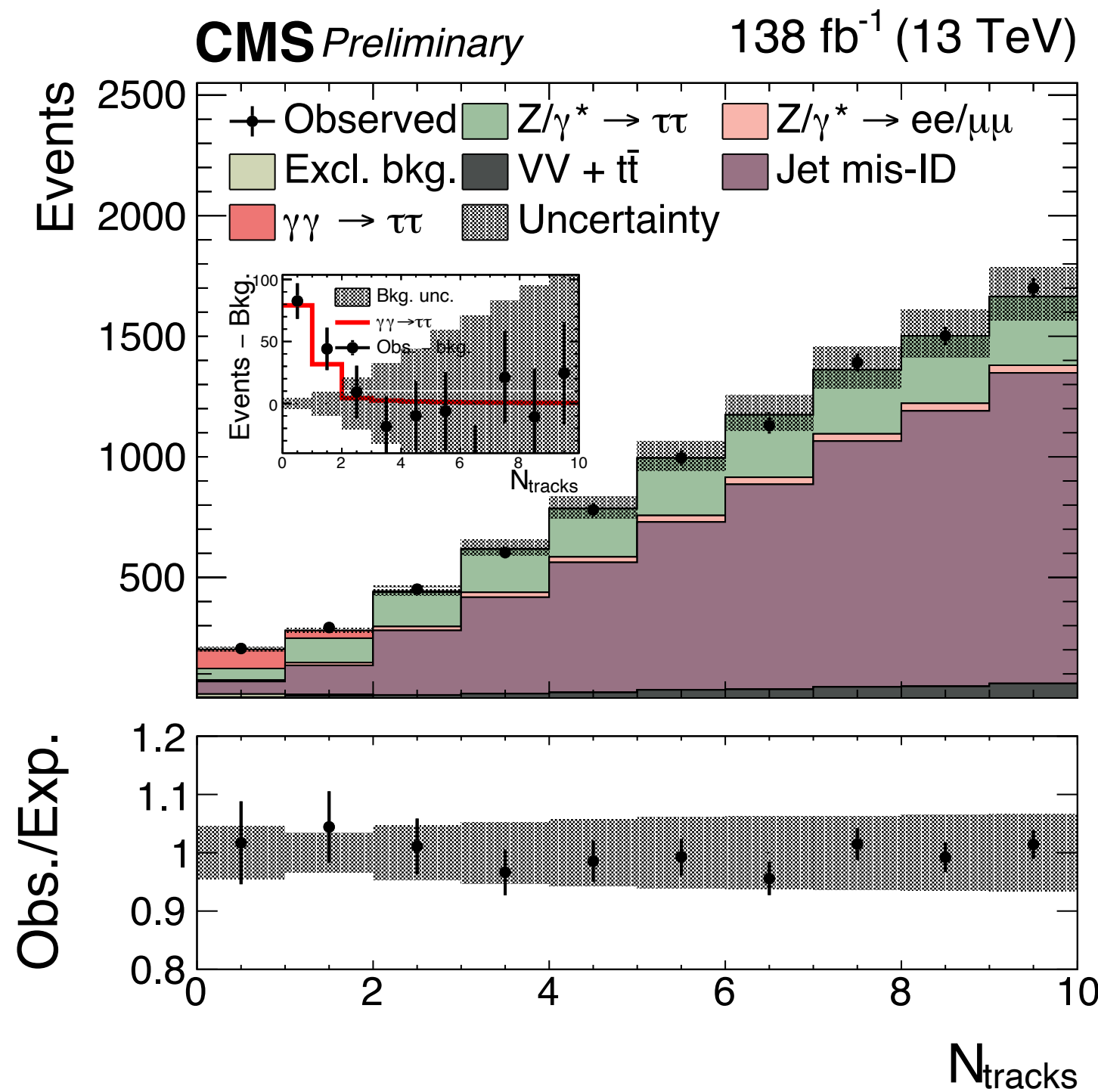
# Summary

- No discovery of resonant new physics at the LHC - (SM)EFT is tool of choice for parameterising effects of heavy new physics on our measurements.
- EFT limits produced from a diverse range of analyses.
  - Number / choice of operators still a challenge.
  - Both strategies of fitting directly reconstructed level data vs fitting measured cross-section have been deployed.
- EWPO + Higgs + diboson global EFT fit done by ATLAS in 2022.
  - Many new results since then -> stay tuned!

# Backup

# CMS $\gamma\gamma \rightarrow \tau\tau$

- N(tracks) distribution without selection, but with  $m_{\text{vis}} > 100$  GeV:



[CMS-PAS-SMP-23-005](#)

# CMS tt + leptons

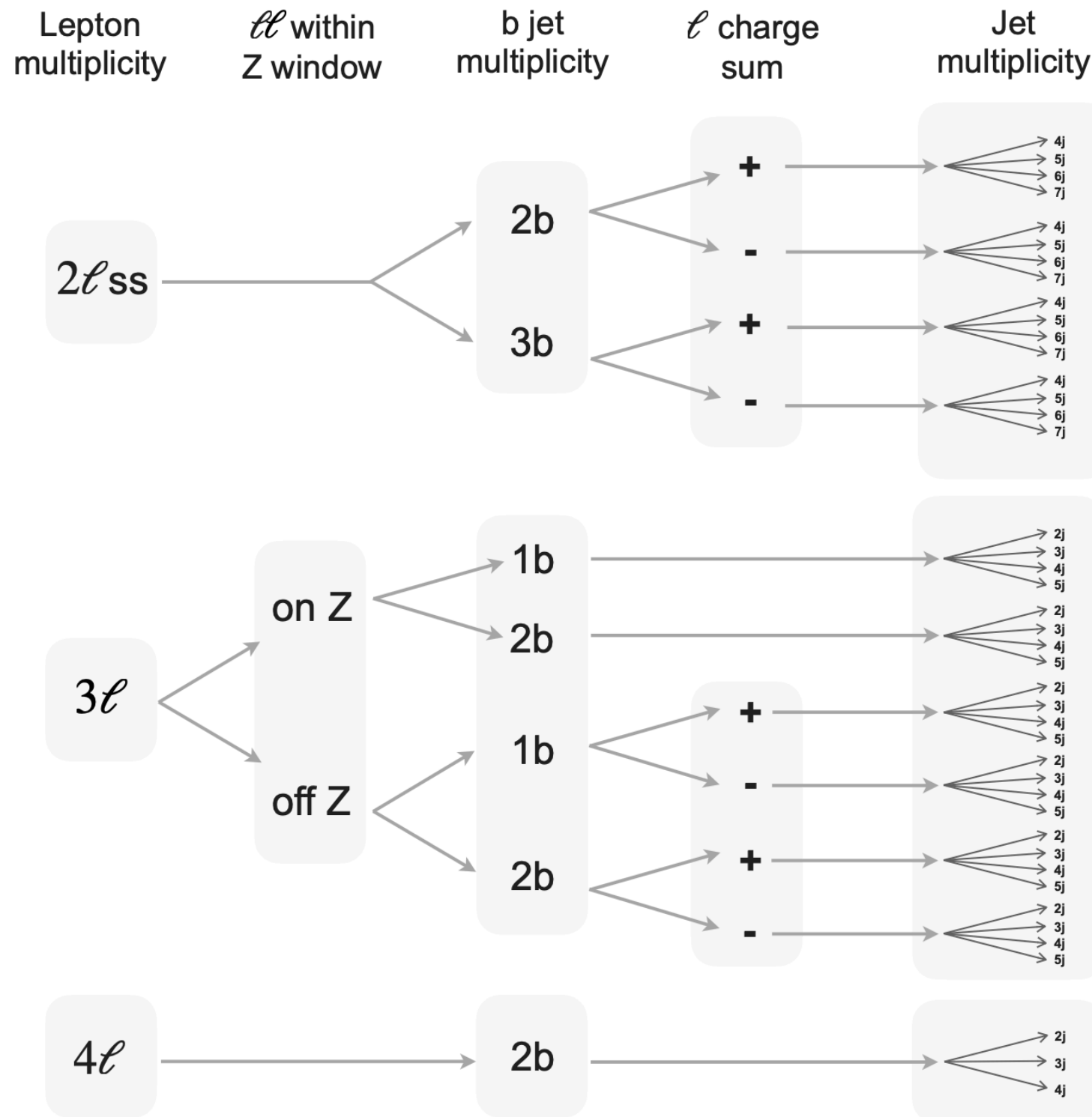
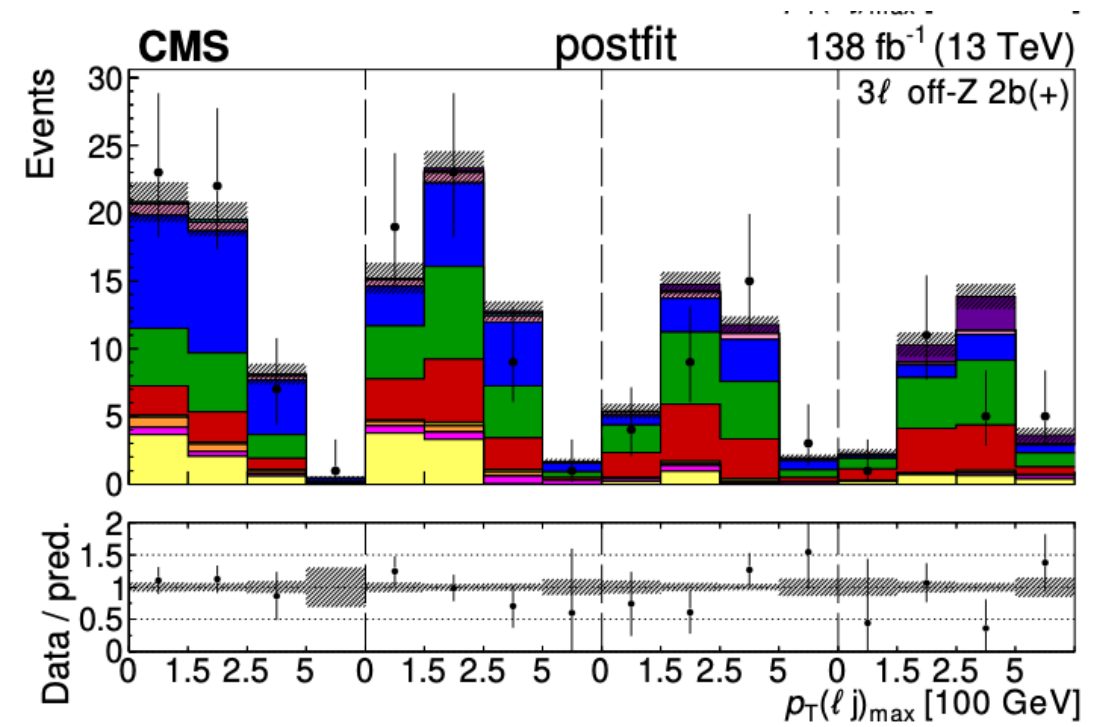
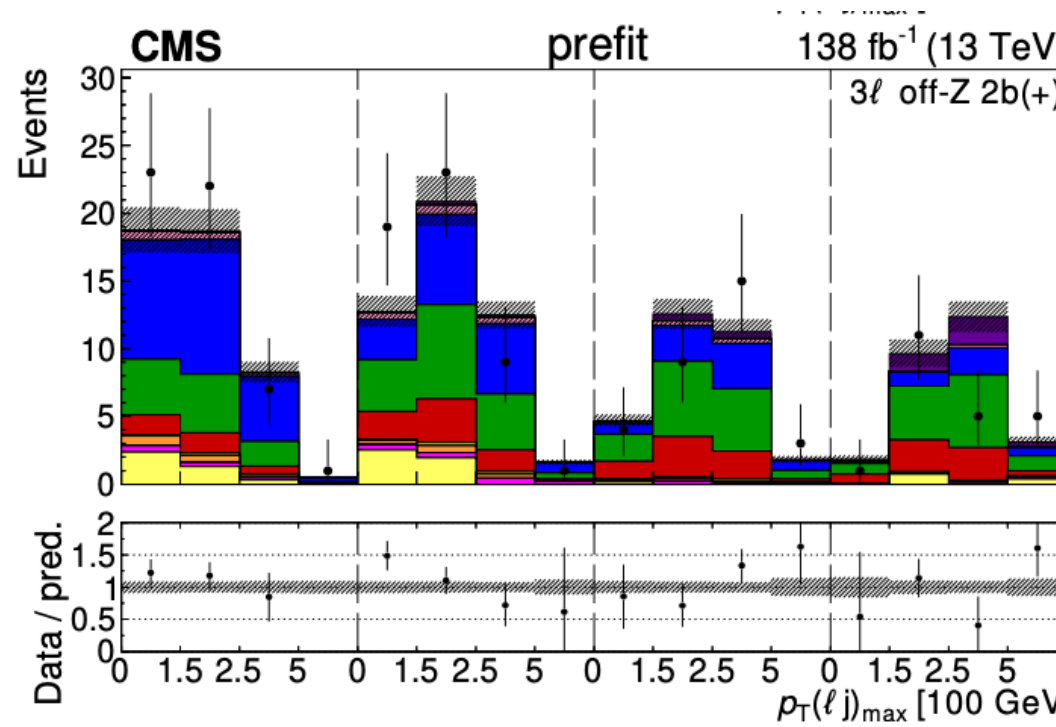
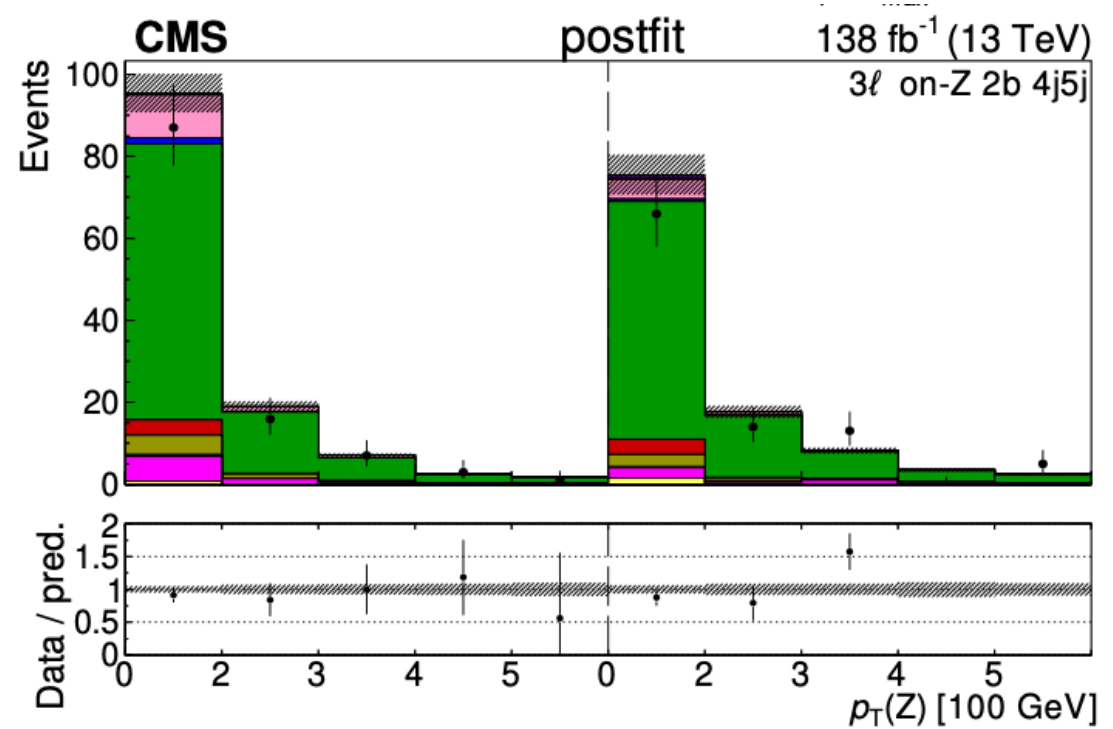
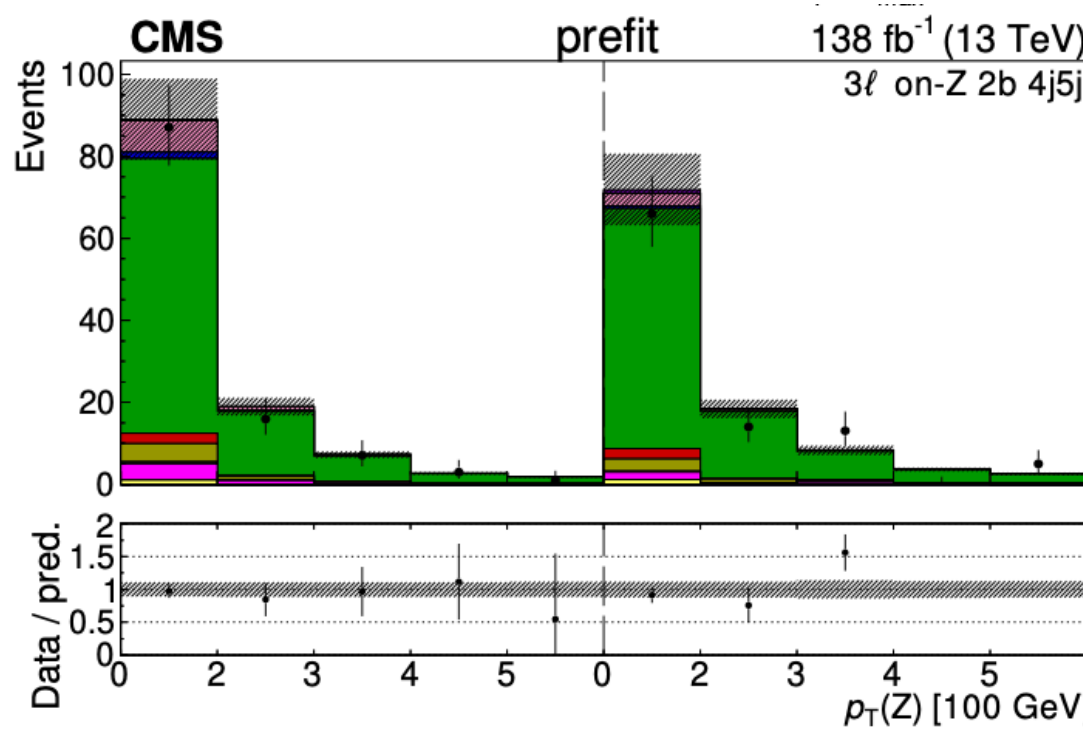


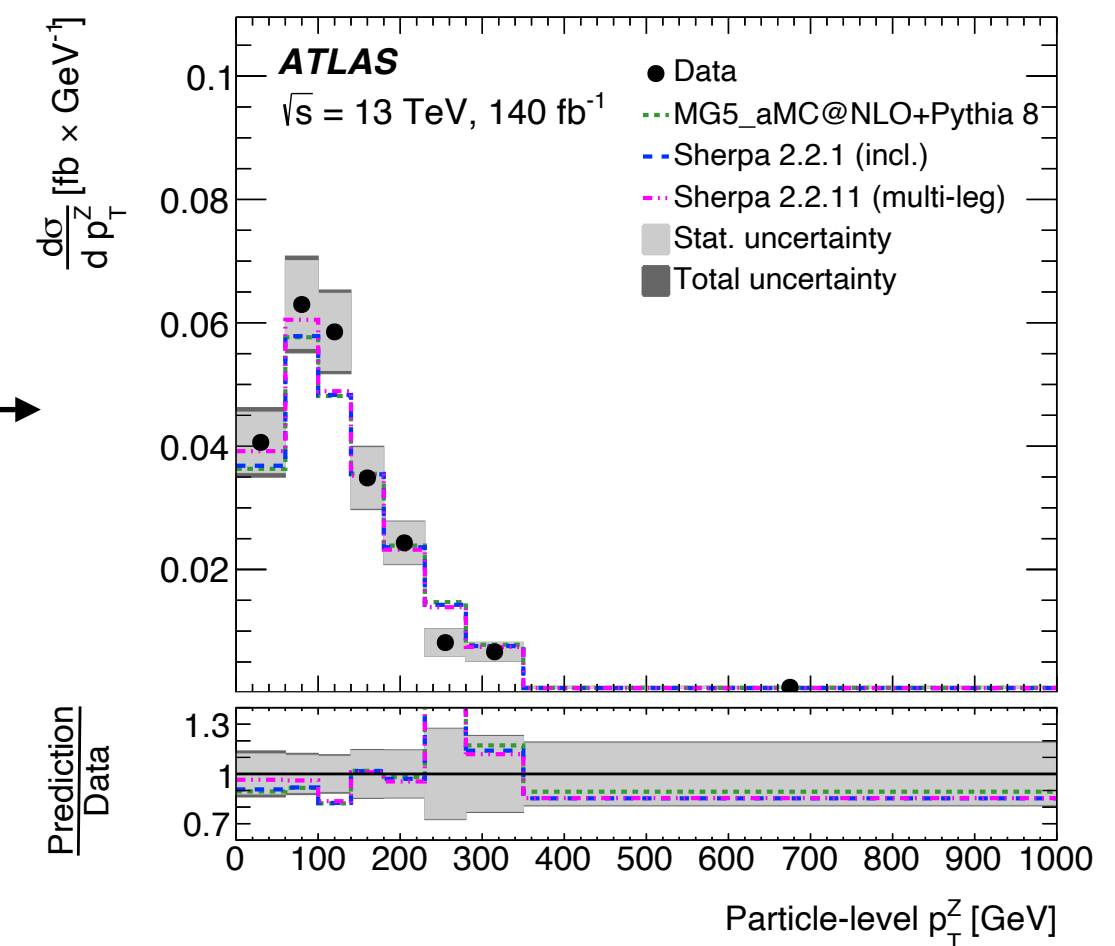
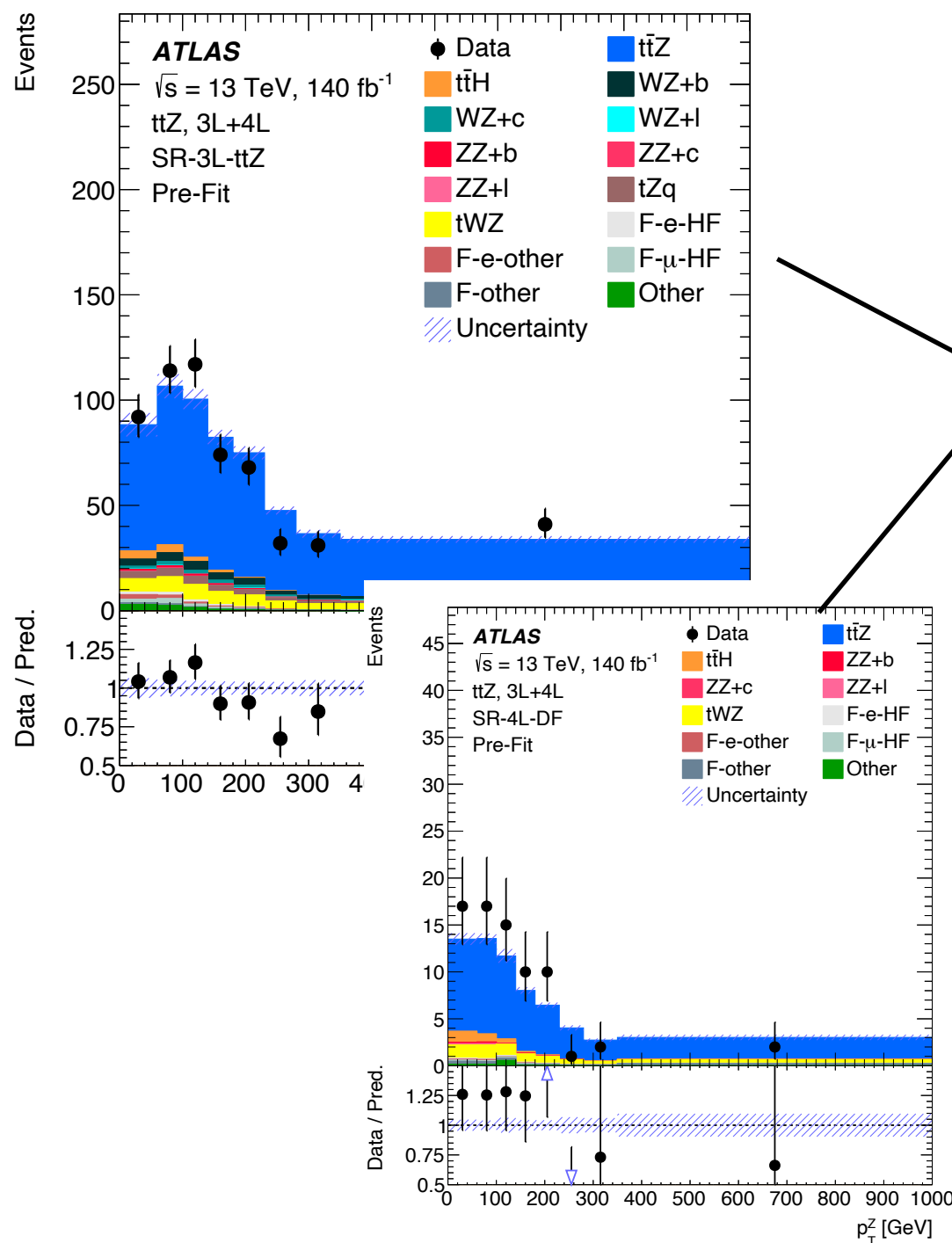
Figure 2: Summary of the event selection categorization. The details for the selection requirements are described in Sections 5.1–5.3.

# CMS tt + leptons



# ATLAS ttZ measurement

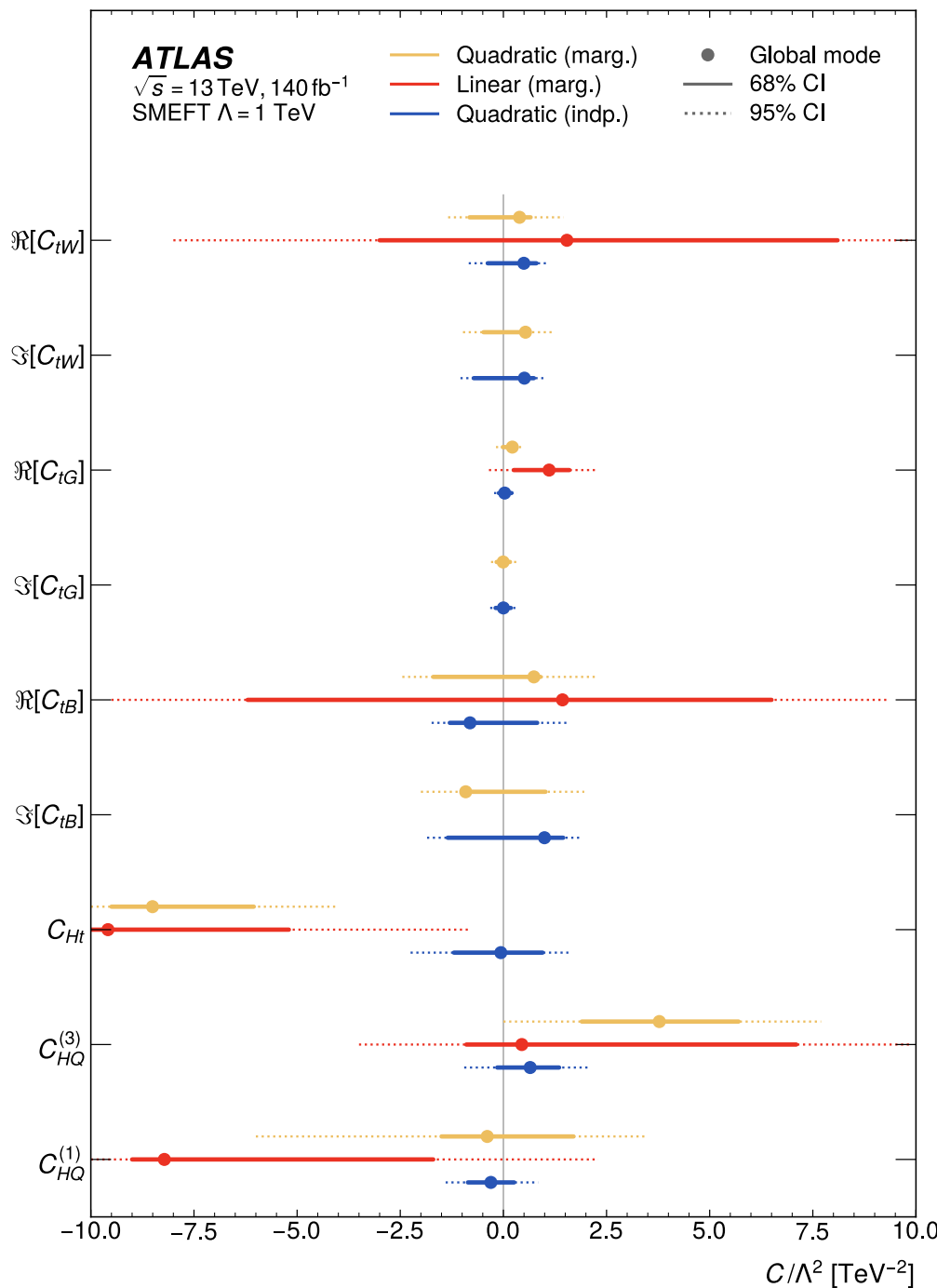
- Recent differential cross-section of  $t\bar{t}Z$  production:



Simultaneous EFT fit to four differential distributions, considering either 6 top-boson, or 14 four-quark operators

# ATLAS ttZ measurement

- Results for top-Boson operators:

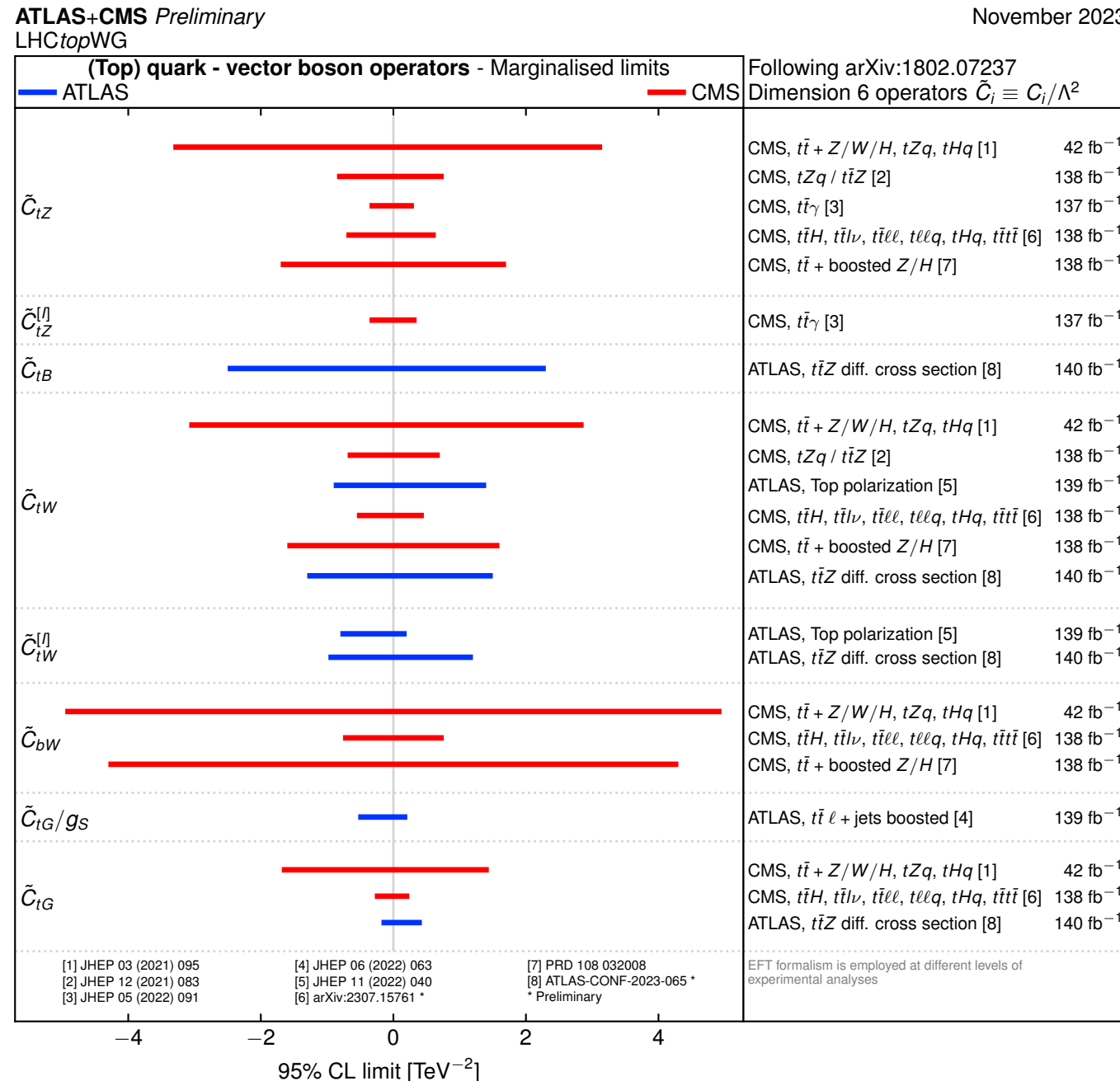


Strong constraints when allowing only one operator to be non-zero (independent, blue).

Weaker constraints once all operators are non-zero (marginalised, yellow).

# Comparing ATLAS and CMS for ttZ

- Very different analysis strategies - would like to compare:



- Unfortunate difference between ATLAS and CMS for definition of top-Z operators:

$$c_{tZ} = -\sin \theta_W C_{tB} + \cos \theta_W C_{tW},$$

$$c_{\varphi Q}^- = C_{HQ}^{(1)} - C_{HQ}^{(3)},$$

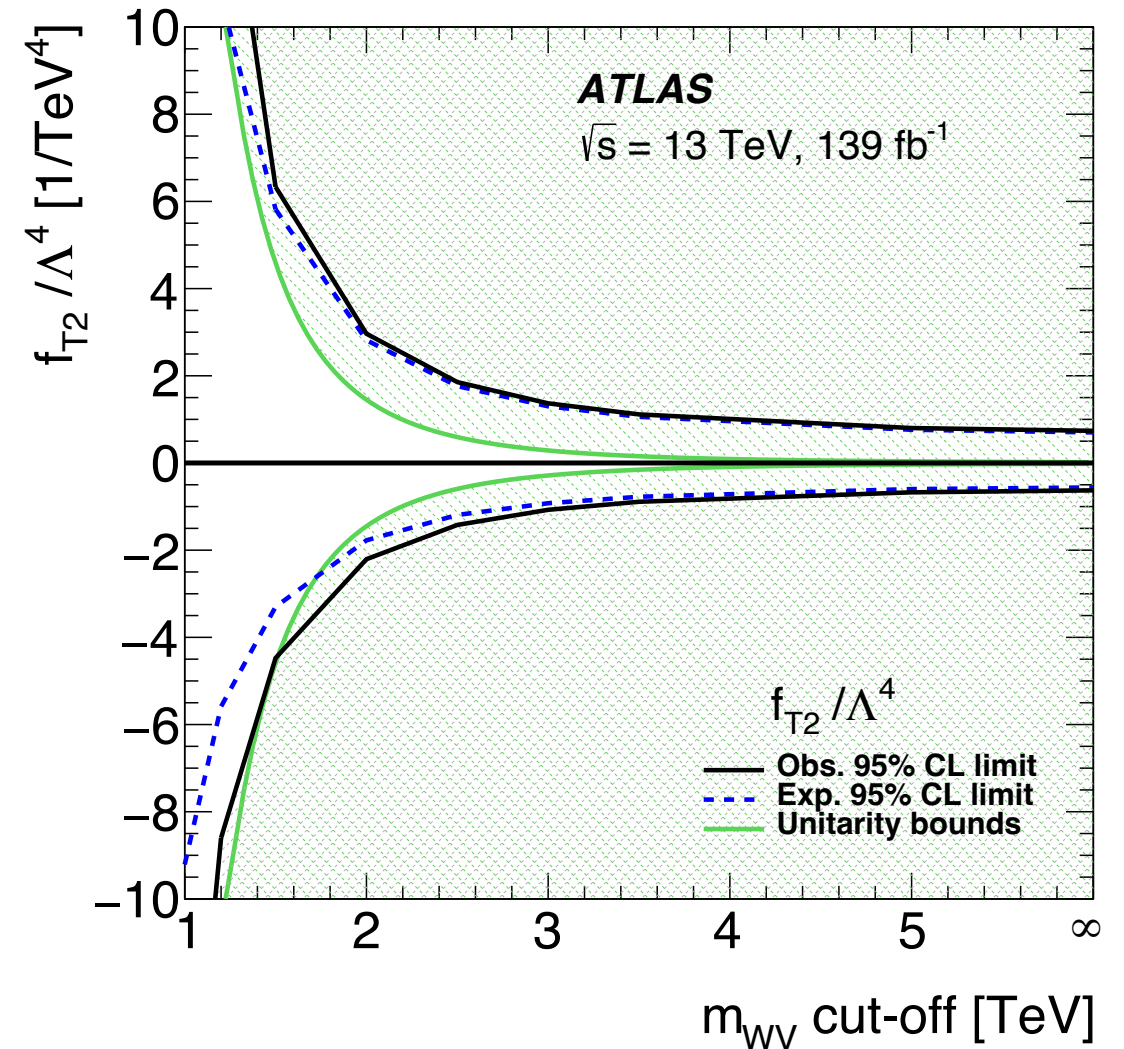
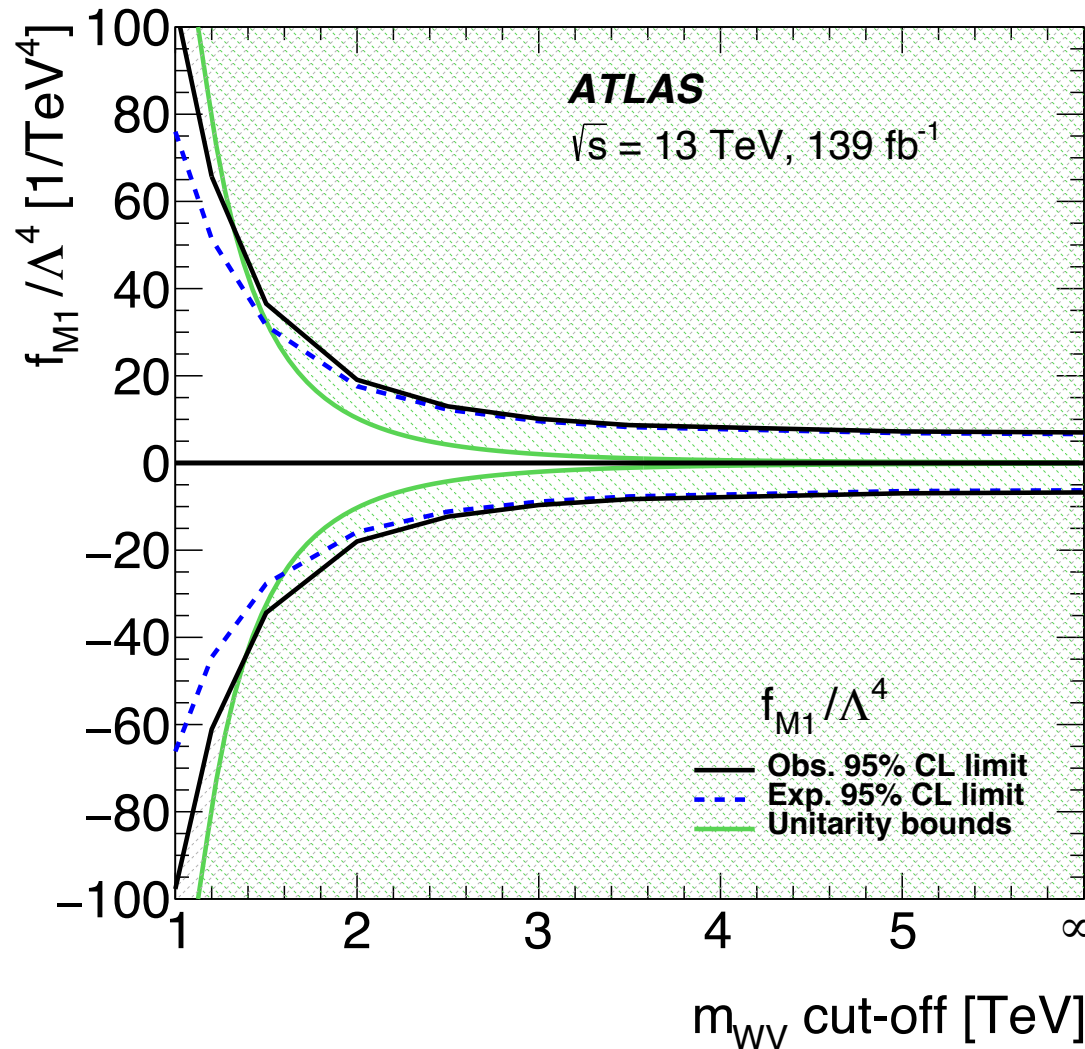
- Would be good to harmonise.

# ATLAS $W^\pm W^\pm jj$

- Operators:
  - $O_{S0,1,2}$ : four covariant derivatives of the Higgs field.
  - $O_{M0,1,7}$ : two Higgs field covariant derivatives, two field-strength tensors.
  - $O_{T0,1,2}$ : four field-strength tensors.
  - $O_{S0}, O_{S2}$  are hermitian conjugate, so assume  $f_{S0} = f_{S2} = f_{S02}$

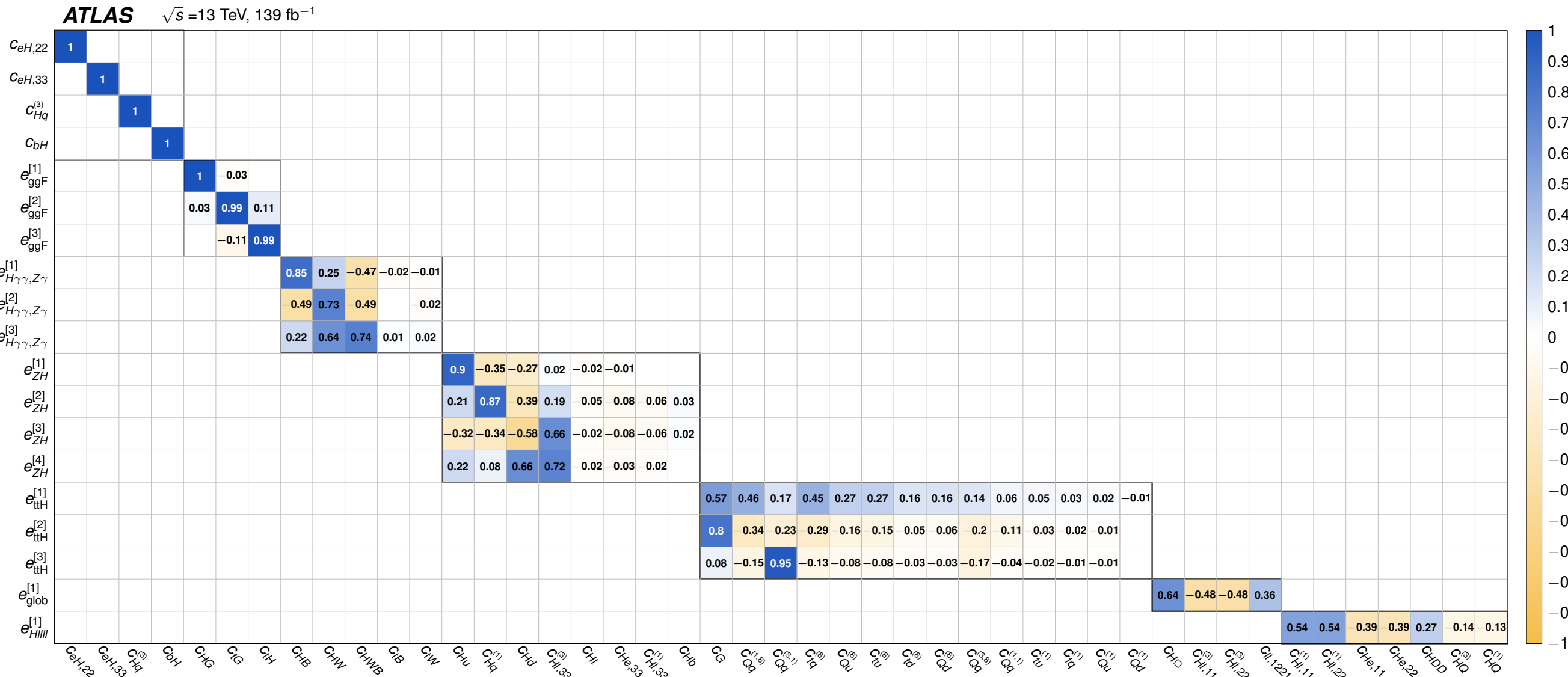
# ATLAS $W^\pm W^\pm jj$

- Unitarity bounds:



# ATLAS Higgs EFT

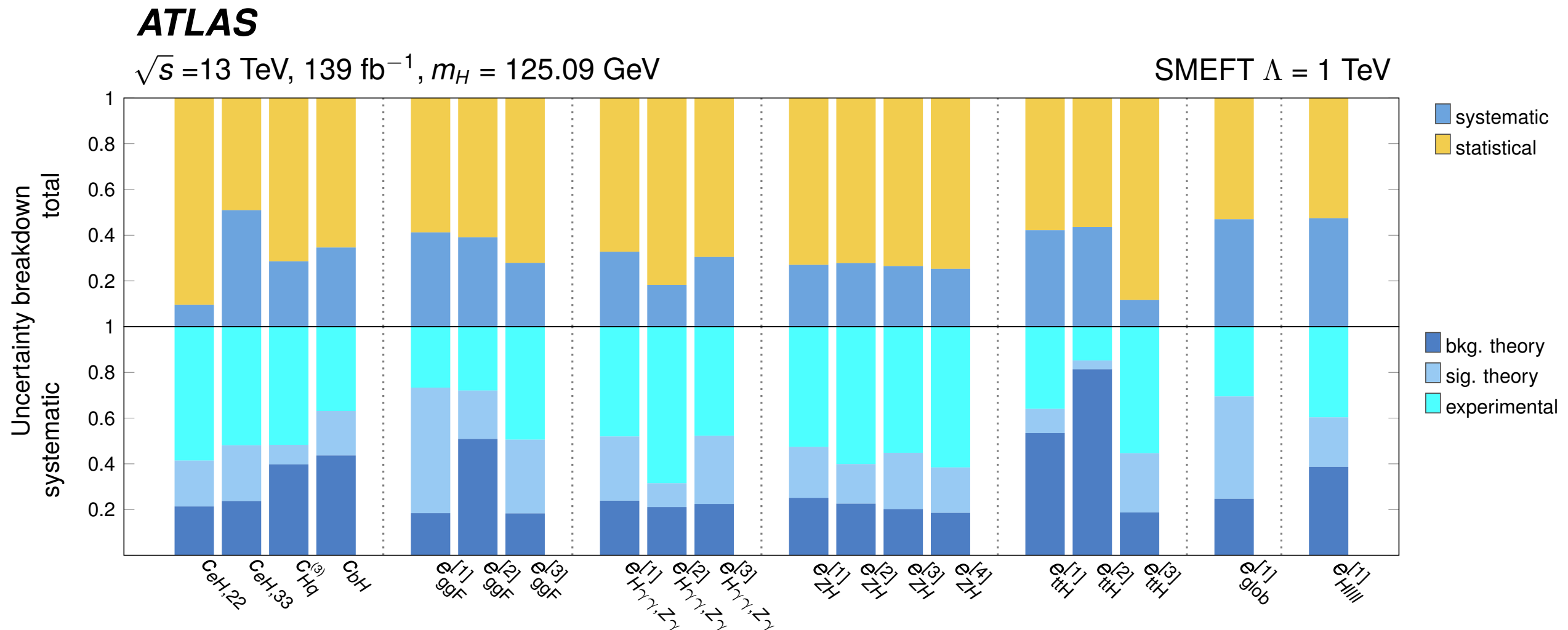
- Eigen-vector basis:



arXiv:2402.05742

# ATLAS Higgs EFT

- Relative importance of statistical and systematic uncertainties:

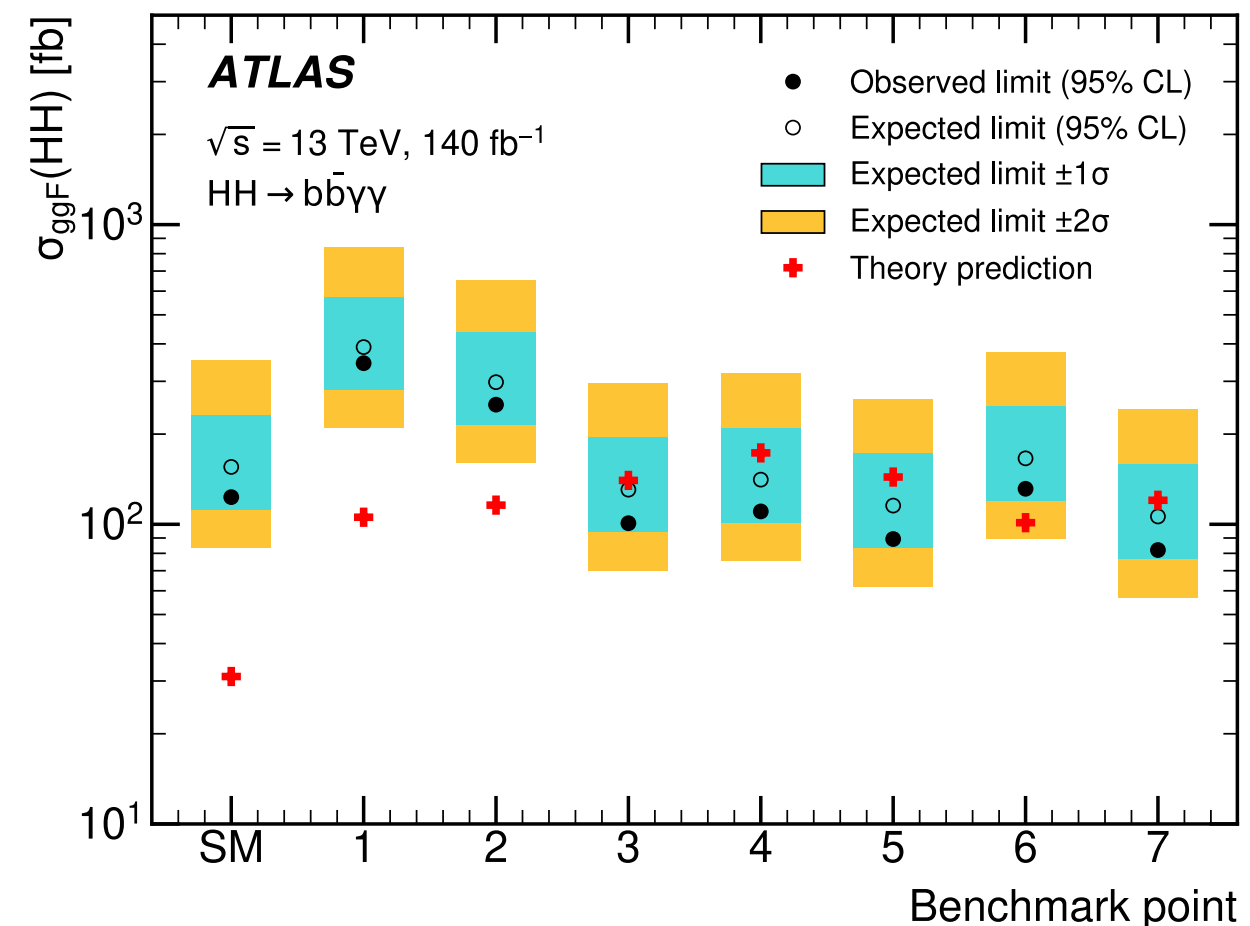


arXiv:2402.05742

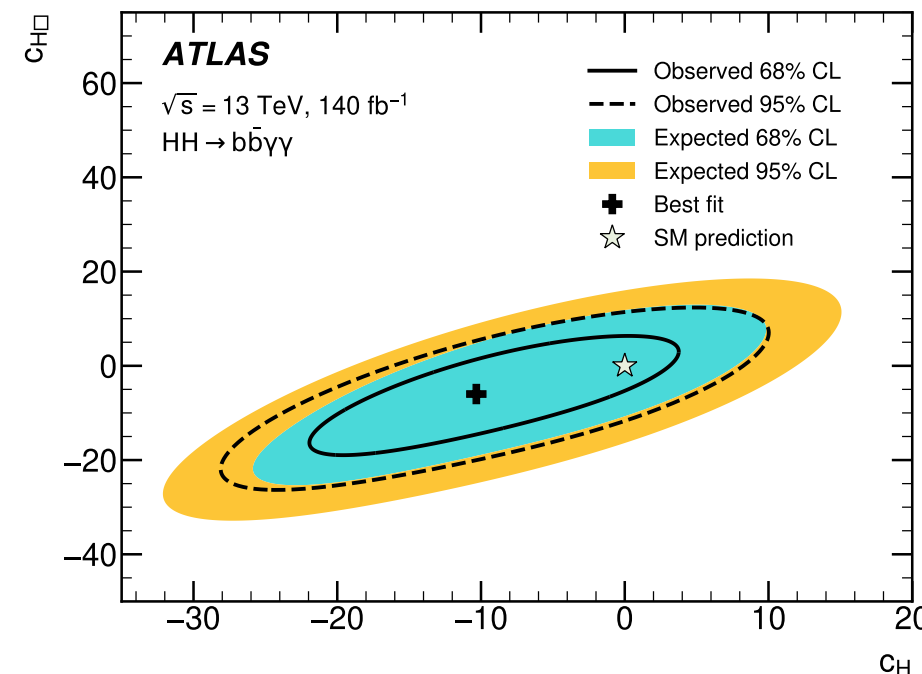
# ATLAS $hh \rightarrow b\bar{b}\gamma\gamma$

- Limits on benchmark HEFT points:

| Benchmark | $c_{hhh}$ | $c_{tth}$ | $c_{ggh}$ | $c_{gghh}$ | $c_{ttth}$ |
|-----------|-----------|-----------|-----------|------------|------------|
| SM        | 1.00      | 1.00      | 0         | 0          | 0          |
| 1         | 5.11      | 1.10      | 0         | 0          | 0          |
| 2         | 6.84      | 1.03      | -1/3      | 0          | 1/6        |
| 3         | 2.21      | 1.05      | 1/2       | 1/2        | -1/3       |
| 4         | 2.79      | 0.90      | -1/3      | -1/2       | -1/6       |
| 5         | 3.95      | 1.17      | 1/6       | -1/2       | -1/3       |
| 6         | -0.68     | 0.90      | 1/2       | 1/4        | -1/6       |
| 7         | -0.10     | 0.94      | 1/6       | -1/6       | 1          |

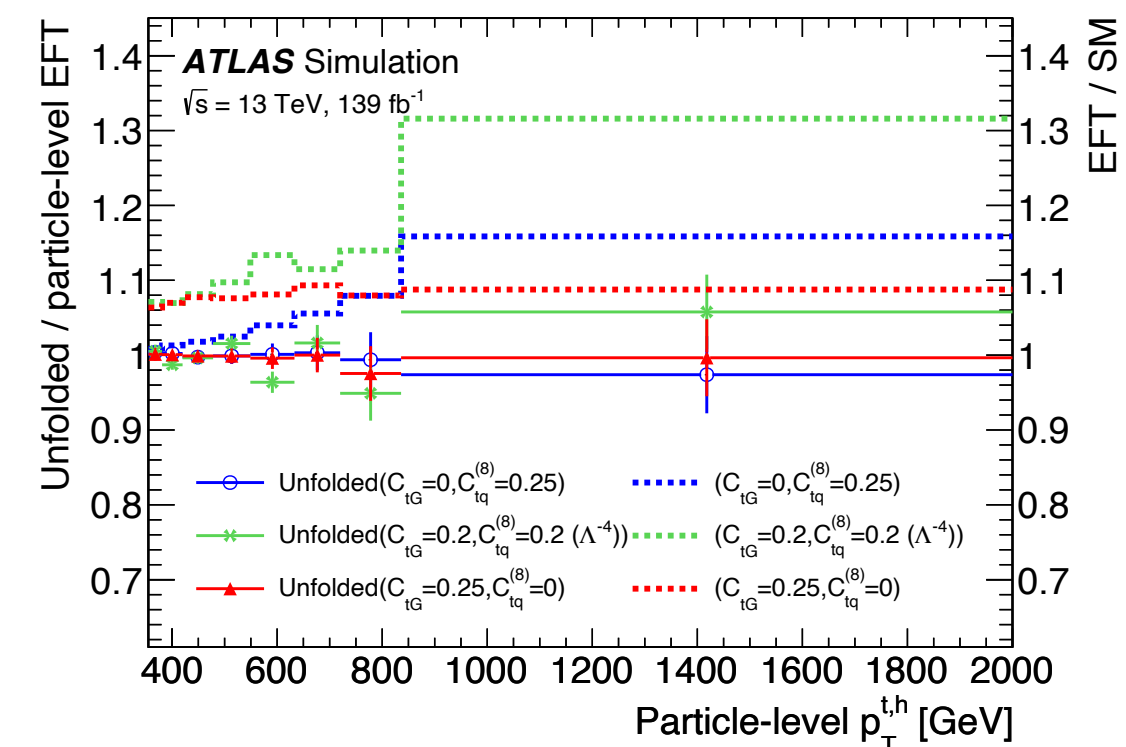
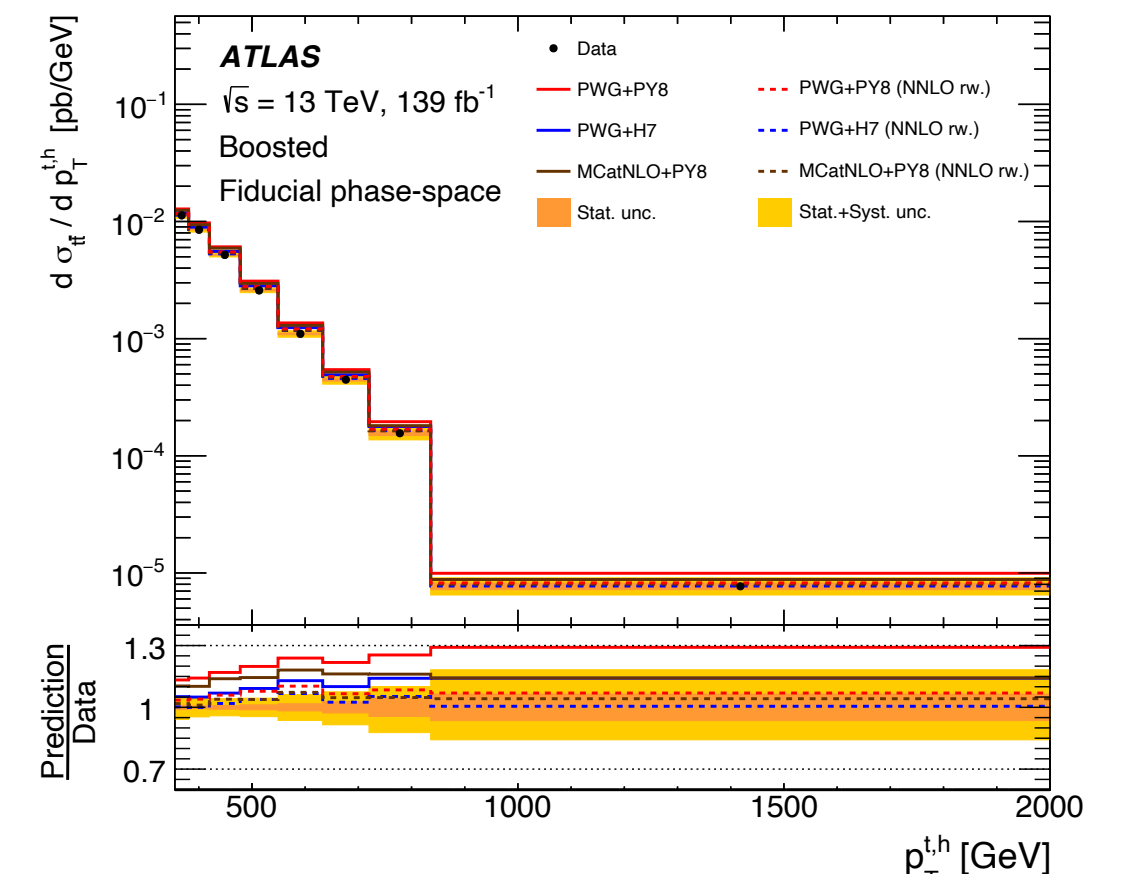
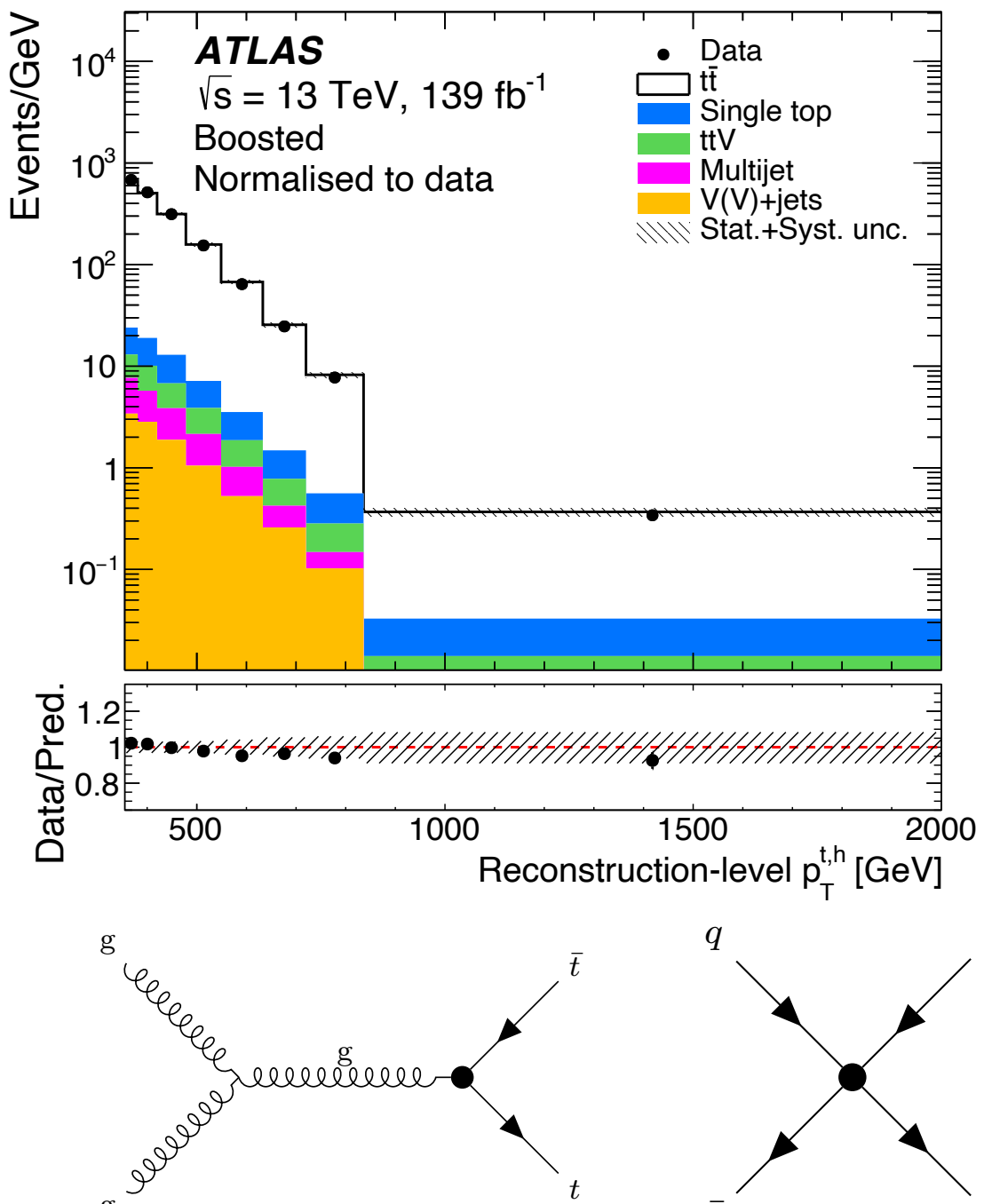


- Limits on benchmark SMEFT:



# ATLAS Boosted top

- Example of closure test with EFT injection:



# ATLAS Boosted top

- Importance of differential information and difference between linear / quadratic terms:

